Drought, agricultural adaptation and sociopolitical collapse in the Maya Lowlands

Peter M. J. Douglas[1*†], Mark Pagani[1], Marcello A. Canuto[2], Mark Brenner[3], David A. Hodell[4], Timothy I. Eglinton[5,6], Jason H. Curtis[3]

For submission to Proceedings of the National Academy of Sciences

[1]Department of Geology and Geophysics, Yale University, New Haven, CT, USA

[2]Middle American Research Institute, Tulane University, New Orleans, LA, USA

[3]Department of Geological Sciences & Land Use and Environmental Change Institute, University of Florida, Gainesville, FL, USA

[4]Godwin Laboratory for Paleoclimate Research, Department of Earth Sciences, Cambridge University, Cambridge, UK

[5]Department of Marine Chemistry and Geochemistry, Woods Hole Oceanographic Institution, Woods Hole, MA, USA

[6]Geological Institute, ETH Zurich, Zurich, Switzerland

[*]Corresponding Author: pdouglas@caltech.edu

[†]Now at Division of Geological and Planetary Sciences, California Institute of Technology, Pasadena, CA, USA

Abstract: Paleoclimate records indicate a series of severe droughts was associated with societal collapse of the Classic Maya during the Terminal Classic period (approximately 800 to 950 CE). Evidence for drought largely derives from the drier, less populated northern Maya Lowlands, but does not explain more pronounced and earlier societal disruption in the relatively humid southern Maya Lowlands. Here we apply hydrogen and carbon isotope compositions of plant-wax lipids in two lake sediment cores to assess changes in water availability and land use in both the northern and southern Maya lowlands. We show that relatively more intense drying occurred in the southern lowlands than in the northern lowlands during the Terminal Classic period, consistent with earlier and more persistent societal decline in the south. Our results also indicate a period of substantial drying in the southern Maya Lowlands from ~200 to 500 CE, during the Terminal Preclassic and Early Classic periods. Plant-wax carbon isotope records indicate a decline in C_4 plants in both lake catchments during the Early Classic period, interpreted to reflect a shift from extensive agriculture to intensive, water-conservative maize cultivation that was motivated by a drying climate. Our results imply that agricultural adaptations developed in response to earlier droughts were initially successful, but failed under the more severe droughts of the Terminal Classic period.

Significance Statement: The Terminal Classic decline of the Maya civilization represents a key example of ancient societal collapse that may have been caused by climate change, but there are inconsistencies between paleoclimate and archaeological evidence regarding the spatial distribution of droughts and sociopolitical disintegration. We conducted a new analysis of regional drought intensity that shows drought was most severe in the region with the strongest societal collapse. We also found that an earlier drought interval coincided with agricultural intensification, suggesting that the ancient Maya adapted to previous episodes of climate drying, but could not cope with the more extreme droughts of the Terminal Classic.

\body

The decline of the lowland Classic Maya during the Terminal Classic period (800 to 900/1000 CE) is a preeminent example of societal collapse (1), but its causes have been vigorously debated (2-5). Paleoclimate inferences from lake sediment and cave deposits (6-11) indicate that the Terminal Classic was marked by a series of major droughts, suggesting that climate change destabilized lowland Maya society. Most evidence for drought during the Terminal Classic comes from the northern Maya Lowlands (Fig. 1) (6-8, 10) where societal disruption was less severe than in the southern Maya Lowlands (12, 13). There are fewer paleoclimate records from the southern Maya Lowlands and they are equivocal with respect to the relative magnitude of drought impacts during the Terminal Classic (9, 11, 14). Further, the supposition that hydrological impacts were a primary cause for societal change is often challenged by archaeologists, who stress spatial variability in societal disruption across the region and the complexity of human responses to environmental change (2, 3, 12). The available paleoclimate data, however, do not constrain possible spatial variability in drought impacts (6-11). Arguments for drought as a principal cause for societal collapse have also not considered the potential resilience of the ancient Maya during earlier intervals of climate change (15).

For this study we analyzed coupled proxy records of climate change and ancient land use derived from stable hydrogen and carbon isotope analyses of higher-plant leaf wax lipids (long chain *n*-alkanoic acids) in sediment cores from Lakes Chichancanab and Salpeten, in the northern and southern Maya Lowlands, respectively (Fig. 1). Hydrogen isotope compositions of *n*-alkanoic acids (δD_{wax}) are primarily influenced by the isotopic composition of precipitation and isotopic fractionation associated with evapotranspiration (16). In the modern Maya Lowlands, δD_{wax} is well correlated with precipitation amount and varies by 60‰ across an annual precipitation gradient of 2500 mm (Fig. 2). This modern variability in δD_{wax} is strongly influenced by soil water evaporation (17), and it is possible that changes in potential evapotranspiration could also impact paleo-records. Accordingly, we interpret δD_{wax} values as qualitative records of water availability influenced by both precipitation amount and potential evapotranspiration. These two effects are complementary, since less rainfall and increased evapotranspiration would lead to both increased δD_{wax} values and reduced water resources, and *vice versa*.

Plant-wax carbon isotope signatures ($\delta^{13}C_{wax}$) in sediments from low-elevation tropical environments, including the Maya lowlands, are primarily controlled by the relative abundance of C_3 and C_4 plants (18-20). Ancient Maya land use was the dominant influence on the relative abundance of C_3 and C_4 plants during the late Holocene, because Maya farmers cleared C_3 plant-dominated forests and promoted C_4 grasses, in particular maize (21-24). Thus, we apply $\delta^{13}C_{wax}$ records as an indicator of the relative abundance of C_4 and C_3 plants that reflects past land use change (SI Text). Physiological differences between plant groups also result in differing δD_{wax} values between C_3 trees and shrubs and C_4 grasses (16) and we use $\delta^{13}C_{wax}$ records to correct for the influence of vegetation change on δD_{wax} values (25) ($\delta D_{wax\text{-}corr}$, SI Text, Fig. S1).

Plant waxes have been shown to have long residence times in soils in the Maya Lowlands (26). Therefore, age-depth models for our plant-wax isotope records are based on compound-specific radiocarbon ages (Fig. 3), which align our δD_{wax} records temporally with nearby hydroclimate records derived from other methodologies (26) (SI

Text, Fig. S2). The mean 95% confidence range for the compound-specific age-depth models is 230 years at Lake Chichancanab and 250 years at Lake Salpeten. Given these age uncertainties we focus our interpretation on centennial-scale variability (26). The temporal resolution of our plant-wax isotope records is lower than speleothem-derived climate records (8, 9), but combining plant-wax records from multiple sites allows comparisons of climate change and land use in the northern and southern Maya Lowlands, which would otherwise not be possible. In addition, plant-wax isotope records extend to the Early Preclassic/Late Archaic period (1500 to 2000 BCE), providing a longer perspective on climate change in the Maya Lowlands than most other regional records (6, 8-11).

Results and Discussion

Inter-site comparison of $\delta D_{wax\text{-}corr}$ hydroclimate records

A key strength of δD_{wax} in the Maya Lowlands is the well-defined spatial relationship between sedimentary δD_{wax} and annual precipitation amount in this region (Fig. 2). Evaporative enrichment of soil-water D/H ratios — primarily associated with annual precipitation amount — is thought to be the dominant mechanism for the spatial range in δD_{wax} in the Maya Lowlands (17), while other climate variables explain much less of the variability in δD_{wax} (Fig. S3). In particular, potential evapotranspiration (PET), which can also influence soil-water D/H ratios, varies much less than annual precipitation and has a much lower correlation with δD_{wax} values (Fig. S3). Application of a vegetation correction to δD_{wax} values in modern lake sediments and soils ($\delta D_{wax\text{-}corr}$; SI Text) to account for differences in the apparent D/H fractionation between environmental water and plant waxes in different plant groups (25) improves its correlation with annual precipitation. Residual variance in $\delta D_{wax\text{-}corr}$ values from lake surface sediments and topsoils, on the order of ±10‰ (Fig. 2), could result from site-specific differences in edaphic properties or microclimates that influence evapotranspiration. It is also possible that the incorporation of aged, soil-derived plant waxes into lake surface sediments contributes to scatter in $\delta D_{wax\text{-}corr}$ values, although this process would not influence topsoil samples (26), or that the applied vegetation correction does not fully account for δD_{wax} differences between plant groups. Importantly, $\delta D_{wax\text{-}corr}$ values in surface sediments from Lakes Chichancanab and Salpeten are within error of the mean value for their respective regions, implying that $\delta D_{wax\text{-}corr}$ values at these lakes are not strongly influenced by non-climatic factors. Accordingly, differences in $\delta D_{wax\text{-}corr}$ values between these two lake sediment cores can be used as an indicator of spatial differences in hydroclimate in the Maya Lowlands.

Past variability in $\delta D_{wax\text{-}corr}$ reflects the combined effects of evaporative enrichment of soil and plant water D/H ratios and temporal variability in the isotopic composition of precipitation, which in this region is primarily controlled by the amount effect (8, 27). Past variability in the evaporative enrichment of soil water D/H ratios could be influenced by changes in both precipitation amount and PET. Temperature is the dominant influence on PET (28), however, and we assume based on paleotemperature estimates that both temperature and PET remained relatively constant in this region during the late Holocene (29). Regardless, if PET did vary, it would have impacted ancient Maya water resources by altering the evaporation of soil moisture and water storage reservoirs, and therefore we interpret $\delta D_{wax\text{-}corr}$ values as a qualitative indicator of past water availability. It is also possible that the strength of the amount effect varied between the northern and southern Maya Lowlands, which would lead to differential changes in $\delta D_{wax\text{-}corr}$ in these two regions for a given decrease in rainfall amount. However, the two Global Network of Isotopes in Precipitation stations nearest to the Maya Lowlands (i.e. Veracruz, Mexico and San Salvador, El Salvador) record nearly identical $\delta^{18}O$-precipitation amount slopes (27) and thus suggest that the strength of the amount effect is largely invariant across southern Mexico and Central America.

In contrast to $\delta D_{wax\text{-}corr}$ records, $\delta^{18}O$ values in carbonate shells from lake sediments and in cave carbonate can be strongly impacted by non-climatic factors that influence local hydrology or $^{18}O/^{16}O$ fractionation between water and carbonate (14, 30-32). Thus, although carbonate $\delta^{18}O$ values within an individual lake sediment core or cave speleothem typically provide a robust indicator of past climate change at a given site, these data cannot be readily compared between lakes or caves to determine spatial differences in climatic change. Notably, $\delta^{18}O$ values for the Yok I speleothem in southern Belize (~ -3.4‰) are ^{18}O-enriched relative to $\delta^{18}O$ values for the Chaac speleothem in the northern Yucatan (~-5.4‰) (Fig. 4B). This isotopic difference is unexpected, given the much wetter climate at Yok Balum Cave and relatively small differences in the isotopic composition of precipitation across the region (17). The difference in $\delta^{18}O$ between the two sites is likely the result of combined evaporative and kinetic isotope effects that influence the Yok I record (9), although these isotopic offsets have not been thoroughly examined. As a consequence, comparison of speleothem isotope records does not provide a clear indication of spatial variability in past climate change in the Maya Lowlands. Similar site-specific hydrological influences confound spatial comparisons between lake sediment $\delta^{18}O$ records (14, 33). Therefore, comparative analysis of $\delta D_{wax\text{-}corr}$ records from Lake Chichancanab and Lake Salpeten provide a unique and powerful tool for understanding how hydrological variability across the region impacted the ancient Maya.

Patterns of Hydroclimate Change in the Maya Lowlands

Our results from Lakes Chichancanab and Salpeten confirm the occurrence of severe and extended droughts throughout the Maya Lowlands during the Terminal Classic (Fig. 4A), with the magnitude of $\delta D_{wax\text{-}corr}$ change (~50-60‰) equivalent to the modern range in $\delta D_{wax\text{-}corr}$ from northern Yucatan to southeastern Guatemala (where annual precipitation ranges from 500 to 3300 mm; Fig. 2). Indeed, major droughts inferred from $\delta D_{wax\text{-}corr}$ during the Terminal Classic represent the driest regional conditions of the preceding ~1200 years at Lake Chichancanab and of the preceding ~2500 years at Lake Salpeten. Importantly, our $\delta D_{wax\text{-}corr}$ records further imply that the large, modern precipitation gradient between Lake Chichancanab and Lake Salpeten (~550 mm; Fig. 1) changed significantly over time (Fig. 5) and that the hydrologic differences between the northern and southern Maya Lowlands effectively collapsed during the Terminal Classic (Fig. 5), with substantially greater drying in the southern lowlands relative to the northern lowlands (Fig. 4).

Differential patterns of paleo-hydroclimate change between these two sites are consistent with analyses of 20th-century rainfall variability that show poor correlation between the northern Yucatan Peninsula and the southern lowlands south of 17° N (8), Mechanistic explanations for these differences remain unresolved, but two scenarios are plausible. Today, the dry climate of northern Yucatan (Fig. 1) results from atmospheric subsidence related to the descending limb of the Hadley cell (34). A southward shift of the Hadley cell during the Terminal Classic (9, 35) would have caused the region of subsidence to expand to the south, and could have led to a stronger decrease in precipitation in the southern lowlands relative to the northern lowlands.

Alternatively, different sensitivities to past ocean circulation could have played a role. Inter-oceanic temperature gradients between the tropical Atlantic and the eastern tropical Pacific are an important driver of summer rainfall variability in Central America (36, 37), and paleoclimate studies have found evidence for a Pacific influence on hydroclimate in northern Guatemala and other regions of Mesoamerica (38-40). In contrast, recent variability in precipitation across northern Yucatan does not appear to have a consistent relationship with Pacific climate variability (36, 41, 42). Rather, past hydroclimate variability in northern Yucatan appears to be primarily linked to the climate of the North Atlantic (10, 43), and may be influenced by North Atlantic tropical cyclones (44). Paleoclimate data indicate increased El Nino event frequency between ~250 to 1400 CE (45), coinciding with drier and more variable hydroclimate at Lake Salpeten (Fig. 4). We suggest that this change in Pacific climate could have increased drought frequency in the southern Maya lowlands by reducing Atlantic-Pacific temperature gradients, but had a lesser impact in the northern Maya lowlands.

Climate Change and Sociopolitical Responses

Changes in hydrological conditions and sociopolitical evolution appear to be linked on centennial timescales in the southern Maya Lowlands. Our Lake Salpeten $\delta D_{wax\text{-}corr}$ record suggests that the southern Lowlands experienced relatively wet and stable conditions during much of the Middle and Late Preclassic periods (~700 BCE to 200 CE) — times marked by continuous demographic growth and increasing sociopolitical complexity throughout the region. The Middle Preclassic gave rise to the first cities with concentrated populations, writing, and public monuments (46, 47), followed by the rise of hierarchical and centralized states during the Late Preclassic period (48).

Lake Salpeten $\delta D_{wax\text{-}corr}$ values indicate pronounced drying from ~200 to 500 CE, a pattern that is broadly consistent with other hydroclimate records from the southern Maya Lowlands (9, 11). Drying during the Early Classic period is associated with the decline and abandonment of some of the largest Late Preclassic political systems in the 3rd century CE and subsequent political fragmentation in the region (15, 46). During that time, widespread political realignment developed gradually under the strong influence of a foreign power, the central Mexican city of Teotihuacan (49). We suggest that climatological stress disrupted the largest Late Preclassic states, enabling smaller and more resilient polities to grow by using adaptations to more variable conditions, such as water conservation (50).

A negative 35‰ δD shift at the beginning of the Late Classic period (~600 CE) indicates substantially wetter conditions around Lake Salpeten for almost two centuries that coincided with a period of intense architectural construction, political expansion, and resource consumption throughout the southern lowlands, including the rise and expansion of large, centralized political entities such as Calakmul and Tikal (51, 52). Dry conditions returned to the southern lowlands around the beginning of the Terminal Classic period (~800 CE), intensified during the early Postclassic period and ended *ca.* 1300 CE. During this time, political complexity in the southern Maya Lowlands underwent a fitful, but inexorable regional decline (3). Monument building and written inscriptions essentially ceased after 820 CE, and the institution of centralized kingship — the main organizing entity of the southern lowlands throughout the first millennium CE —disappeared forever (5, 53, 54). Importantly, political decline in the southern lowlands during the Terminal Classic differed from that at the end of the Preclassic period, in that it was not followed by the development of new, resilient political centers. We argue that the absence of a significant Postclassic recovery in the southern lowlands was related to the more intense and sustained interval of drought in the region.

Ancient Maya Land Use Change and Climate Adaptation

Ancient lowland Maya populations adapted to available water resources and employed a diverse set of land-use practices (13, 55) that likely preconditioned their vulnerability to hydrological change. While $\delta D_{wax\text{-}corr}$ reflects hydrological conditions, $\delta^{13}C_{wax}$ records reflect the relative proportion of C_3 and C_4 plants in the lake catchment, and thus local agricultural practices (SI Text). During the Preclassic period, C_4 plant abundance in both the Lake Salpeten and Chichancanab catchments was relatively high, with large variability on centennial timescales (Fig. 6A,B). A long-term shift toward fewer C_4 plants occurred at the beginning of the Classic period in both catchments. Relatively low C_4 plant abundance persisted in both catchments into the Early Postclassic, followed by an increase at the end of that period. The inferred decrease in C_4 plant coverage at Lake Salpeten is consistent with pollen records that show decreased grass abundance in the Early Classic period (21) (Fig. S4, SI Text), accompanied by an increase in C_3-plant disturbance taxa (Fig. S4).

The Early Classic trend of decreasing C_4 plant abundance in these two catchments directly coincides with drying trends in both the northern and southern Maya lowlands

(Fig. 6A,B), as well evidence of population growth both locally at Lake Salpeten (56) and across the southern Maya Lowlands regionally (57) (Fig. 6C) during the Classic period. Consequently, it is unlikely that evidence for fewer C_4 plants reflects a regional reduction in maize agriculture. Instead, we argue that increasingly negative $\delta^{13}C_{wax}$ trends mark adaptations of local land-use in response to drier conditions. In both lake catchments, the Preclassic period was likely characterized by widespread application of rain-fed swidden (slash-and-burn) agriculture that promoted maize and other C_4 plant growth. The drier conditions during the Early Classic period would have inhibited swidden agriculture. Geoarchaeological evidence suggests that intensive agricultural strategies were adopted during the Classic period in many areas of the Maya Lowlands (55, 58, 59), possibly in response to limited rainfall (58). We suggest that the growth of population around Lake Salpeten was associated with a reduction in swidden agriculture and its replacement by increased intensive maize cultivation outside the lake catchment in places with reliable water resources, including seasonal and perennial wetlands (58, 59). If local land-use changes in our two studied sites were representative of broader patterns, they imply a shift to spatially concentrated and regionally integrated agricultural economies during the Early Classic period that encouraged the growth of high-density population centers.

Given the Classic period population growth surrounding Lake Salpeten, it appears that such adaptations were an effective response to the drier conditions of the Early Classic period. Further, with the onset of wetter conditions in the Late Classic period, these agricultural strategies would have promoted enhanced population growth and agricultural productivity, contributing to increased sociopolitical centralization and expansion. By increasing societal complexity, however, the organization of lowland

Classic Maya society into large, centralized states could have reduced resilience to the more intense droughts of the Terminal Classic (1).

Conclusions

Carbon and hydrogen isotope compositions of sedimentary leaf waxes from Lakes Chichancanab and Salpeten support the hypothesis that drought was instrumental to the Terminal Classic decline of the Classic Maya throughout the Maya Lowlands. Drying was more intense in the southern lowlands, where societal collapse occurred earliest and was most pronounced and permanent. Our work further suggests that the Maya successfully adapted land-use practices during previous droughts of the Early Classic period, but that more severe droughts during the Terminal Classic, as well as the increased complexity of Late Classic societies, made adaptation to climate change less effective.

Materials and Methods:

Sediment cores and sampling

Lake Chichancanab is an elongate, fault-bounded karst lake located in the interior of the Yucatan Peninsula, Mexico (Fig. 1). The sediment core we analyzed was collected with a piston-corer in 14.5 m of water, in March 2004 (6). Lake Chichancanab sediments are composed primarily of low-density organic-rich gyttja, but possess distinctive intervals of high-density gypsum, deposited during periods of drought (6). δD_{wax} data from this core were reported in Ref. 26; high-resolution $\delta^{13}C_{wax}$ data from this core are presented here for the first time.

Lake Salpeten is one of a series of east-west aligned lakes in central Petén, northern Guatemala. The Lake Salpeten sediment core was collected with a piston-corer in 16 m of water, in August 1999 (14). Uppermost and lowermost sediments from Lake Salpeten are organic-rich gyttja, whereas the central portion of the core is composed of dense clay, thought to be the result of intense soil erosion caused by ancient Maya land clearance (14). This contrasts with Lake Chichancanab, where there is no sedimentological evidence for large-scale soil erosion.

Plant-wax lipid extraction and preparation

Methods for plant-wax lipid extraction and preparation were previously described (26). Briefly, all sediment core samples were freeze-dried and solvent-extracted. Between 0.5 and 23 g dry sediment were extracted per sample. The total lipid extract was then hydrolyzed and acid and neutral fractions were extracted.
The acid fraction of all samples was esterified using 14% boron trifluoride in methanol. The resulting fatty acid methyl esters (FAMEs) were then purified using silica gel chromatography. Purified FAMEs were quantified relative to an external quantitative standard by gas chromatography.

Compound-specific stable isotope analyses

Methods for plant-wax stable isotope analyses were previously described (26). δD and $\delta^{13}C$ values for individual FAMEs were determined by gas chromatography-isotope ratio mass spectrometry (GC-IRMS) at the Yale University Earth System Center for Stable Isotopic Studies. The H_3^+ factor for the GC-IRMS was measured daily prior to δD analysis. External and internal FAME isotope standards were used to standardize and normalize sample isotope values. The precision of the standard analyses was ≤±5‰ for δD analyses and ≤±0.5‰ for $\delta^{13}C$ analyses. Most samples were run in duplicate or triplicate for both hydrogen and carbon isotope analysis, and the reported isotope ratio value is the mean of replicate runs. For some samples, long chain FAME abundances were insufficient for replicate analyses. FAME $\delta^{13}C$ and δD values were corrected for the isotopic composition of the methyl group added during esterification, by measuring a phthalic acid standard of known isotopic composition esterified in the same manner as the samples. δD_{wax} and $\delta^{13}C_{wax}$ values were calculated as the unweighted mean isotopic composition of the n-C_{26}, n-C_{28}, and n-C_{30} alkanoic acid homologs (SI Text, Tables S1 and S2).

Compound-specific radiocarbon analyses of plant-wax lipids

Methods for plant-wax radiocarbon analyses are described in Ref. 26. Long-carbon-chain-length FAMEs were isolated using a Preparative Capillary Gas Chromatography (PCGC) system at either the Woods Hole Oceanographic Institution Department of Marine Chemistry and Geochemistry or the National Ocean Sciences Accelerator Mass Spectrometry Facility (60). Individual FAMES were not sufficiently abundant for $\Delta^{14}C$ analysis, so we combined four long-chain n-alkanoic acid homologs (C_{26}, $C_{28,}$ C_{30}, and C_{32}). Isolated FAME fractions were quantified and checked for purity using GC-FID. The samples were transferred to pre-combusted quartz tubes, all solvent was evaporated under nitrogen, and the samples were combusted in the presence of cupric oxide at 850°C to yield CO_2. The resulting CO_2 was quantified and purified, and then reduced to graphite and analyzed for radiocarbon content at the NOSAMS facility. Compound-specific radiocarbon results were corrected for procedural blanks by accounting for the blank contribution determined using the same analytical protocol and equipment (61). A sample of the methanol used for esterification was analyzed for $\Delta^{14}C$ at NOSAMS, and FAME $\Delta^{14}C$ values were corrected for the addition of methyl carbon.

$\Delta^{14}C_{wax}$ results from Lake Chichancanab were initially reported in Ref. 26; $\Delta^{14}C_{wax}$ results from Lake Salpeten are reported for the first time here (Table S3).

Age-depth models

The development of terrigenous-macrofossil (TM) and plant-wax (PW) age-depth models for Lake Chichancanab are described in Ref. 26. We employed a similar approach to define TM and PW age-depth models for Lake Salpeten. Specifically, we developed a linear-interpolated age-depth PW age model for Lake Salpeten using the Classical Age-depth Modeling (CLAM v2.2) software in R (62). We also recalculated the 4th-order polynomial TM age-depth model for Lake Salpeten (14) using CLAM. All ^{14}C ages were calibrated to calendar ages using the IntCal13 calibration (63).

Acknowledgments Gerard Olack, Glendon Hunsinger, and Dominic Colosi provided assistance with compound-specific stable isotope measurements, and Daniel Montluçon, Li Xu, and Ann McNichol provided assistance with compound specific radiocarbon measurements. Hagit Affek provided helpful comments on an earlier version of the manuscript and two anonymous reviewers provided constructive commentary. This work was partially funded by the Italian Ministry of the Environment and by the U.S. National Science Foundation Graduate Research Fellowship.

References

1. Tainter J (1990) *The collapse of complex societies* (Cambridge University Press, Cambridge).
2. Aimers JJ (2007) What Maya collapse? Terminal classic variation in the Maya lowlands. *Journal of Archaeological Research* 15(4):329-377.

3. Demarest AA & Rice DS eds (2005) *The Terminal Classic in the Maya Lowlands: Collapse, Transition, and Transformation* (University Press of Colorado, Boulder).
4. Iannone G ed (2014) *The Great Maya Droughts in Cultural Context* (University Press of Colorado, Boulder).
5. Yaeger J & Hodell DA (2008) The Collapse of Maya Civilization: Assessing the Interaction of Culture, Climate, and Environment. *El Niño, Catastrophism, and Culture Change*, eds Sandweiss DH & Quilter J (Dumbarton Oaks, Washington, D.C.), pp 187-242.
6. Hodell DA, Brenner M, & Curtis JH (2005) Terminal Classic drought in the northern Maya lowlands inferred from multiple sediment cores in Lake Chichancanab (Mexico). *Quaternary Sci Rev* 24(12-13):1413-1427.
7. Hodell DA, Curtis JH, & Brenner M (1995) Possible Role of Climate in the Collapse of Classic Maya Civilization. *Nature* 375(6530):391-394.
8. Medina-Elizalde M*, et al.* (2010) High resolution stalagmite climate record from the Yucatan Peninsula spanning the Maya terminal classic period. *Earth Planet Sc Lett* 298(1-2):255-262.
9. Kennett DJ*, et al.* (2012) Development and Disintegration of Maya Political Systems in Response to Climate Change. *Science* 338(6108):788-791.
10. Curtis JH, Hodell DA, & Brenner M (1996) Climate variability on the Yucatan Peninsula (Mexico) during the past 3500 years, and implications for Maya Cultural Evolution. *Quaternary Res* 46(1):37-47.
11. Webster JW*, et al.* (2007) Stalagmite evidence from Belize indicating significant droughts at the time of Preclassic Abandonment, the Maya Hiatus, and the Classic Maya collapse. *Palaeogeogr Palaeocl* 250(1-4):1-17.
12. Dahlin BH (2002) Climate change and the end of the Classic Period in Yucatan: Resolving a paradox. *Ancient Mesoamerica* 13:327-340.
13. Turner B & Sabloff JA (2012) Classic Period collapse of the Central Maya Lowlands: Insights about human–environment relationships for sustainability. *Proceedings of the National Academy of Sciences* 109(35):13908-13914.
14. Rosenmeier MF, Hodell DA, Brenner M, Curtis JH, & Guilderson TP (2002) A 4000-year lacustrine record of environmental change in the southern Maya lowlands, Peten, Guatemala. *Quaternary Res* 57(2):183-190.
15. Dunning N*, et al.* (2014) The End of the Beginning: Drought, Environmental Change and the Preclassic to Classic Transition in the East Central Maya Lowlands. *The Great Maya Droughts in Cultural Context: Case Studies in Resilience and Vulnerability*, ed Iannone G (University Press of Colorado, Boulder), pp 107-126.
16. Sachse D*, et al.* (2012) Molecular paleohydrology: Interpreting the hydrogen-isotopic composition of lipid biomarkers from photosynthesizing organisms. *Annual Review of Earth and Planetary Sciences* 40:221-249.
17. Douglas PMJ, Pagani M, Brenner M, Hodell DA, & Curtis JH (2012) Aridity and vegetation composition are important determinants of leaf-wax δD values in southeastern Mexico and Central America. *Geochim Cosmochim Ac* 97:24-45.

18. Huang Y, *et al.* (2001) Climate change as the dominant control on glacial-interglacial variations in C_3 and C_4 plant abundance. *Science* 293(5535):1647-1651.

19. Hughen KA, Eglinton TI, Xu L, & Makou M (2004) Abrupt tropical vegetation response to rapid climate changes. *Science* 304(5679):1955-1959.

20. Huang YS, Dupont L, Sarnthein M, Hayes JM, & Eglinton G (2000) Mapping of C_4 plant input from North West Africa into North East Atlantic sediments. *Geochim Cosmochim Ac* 64(20):3505-3513.

21. Leyden BW (1987) Man and Climate in the Maya Lowlands. *Quaternary Res* 28(3):407-417.

22. Leyden BW (2002) Pollen evidence for climatic variability and cultural disturbance in the Maya lowlands. *Ancient Mesoamerica* 13:85-101.

23. Wahl D, Byrne R, Schreiner T, & Hansen R (2006) Holocene vegetation change in the northern Peten and its implications for Maya prehistory. *Quaternary Res* 65(3):380-389.

24. Beach T, *et al.* (2011) Carbon isotopic ratios of wetland and terrace soil sequences in the Maya Lowlands of Belize and Guatemala. *Catena* 85(2):109-118.

25. Collins JA, *et al.* (2013) Estimating the hydrogen isotopic composition of past precipitation using leaf-waxes from western Africa. *Quaternary Sci Rev* 65:88-101.

26. Douglas PM, *et al.* (2014) Pre-aged plant waxes in tropical lake sediments and their influence on the chronology of molecular paleoclimate proxy records. *Geochim Cosmochim Ac* 141:346-364.

27. Lachniet MS & Patterson WP (2009) Oxygen isotope values of precipitation and surface waters in northern Central America (Belize and Guatemala) are dominated by temperature and amount effects. *Earth Planet Sc Lett* 284(3-4):435-446.

28. Rind D, Goldberg R, Hansen J, Rosenzweig C, & Ruedy R (1990) Potential evapotranspiration and the likelihood of future drought. *Journal of Geophysical Research: Atmospheres* 95:9983-10004.

29. Hodell DA, *et al.* (2012) Late Glacial temperature and precipitation changes in the lowland Neotropics by tandem measurement of $\delta^{18}O$ in biogenic carbonate and gypsum hydration water. *Geochim Cosmochim Ac* 77:352-368.

30. Henderson AK & Shuman BN (2009) Hydrogen and oxygen isotopic compositions of lake water in the western United States. *Geological Society of America Bulletin* 121(7-8):1179-1189.

31. Lachniet MS (2009) Climatic and environmental controls on speleothem oxygen-isotope values. *Quaternary Sci Rev* 28(5):412-432.

32. Kluge T & Affek HP (2012) Quantifying kinetic fractionation in Bunker Cave speleothems using Δ_{47}. *Quaternary Sci Rev* 49:82-94.

33. Curtis JH, *et al.* (1998) A multi-proxy study of Holocene environmental change in the Maya lowlands of Peten, Guatemala. *J Paleolimnol* 19(2):139-159.

34. Waliser DE, Shi Z, Lanzante J, & Oort A (1999) The Hadley circulation: assessing NCEP/NCAR reanalysis and sparse in-situ estimates. *Clim Dynam* 15(10):719-735.

35. Haug GH, *et al.* (2003) Climate and the collapse of Maya civilization. *Science* 299(5613):1731-1735.
36. Giannini A, Kushnir Y, & Cane MA (2000) Interannual variability of Caribbean rainfall, ENSO, and the Atlantic Ocean. *J Climate* 13(2):297-311.
37. Taylor MA, Stephenson TS, Owino A, Chen AA, & Campbell JD (2011) Tropical gradient influences on Caribbean rainfall. *Journal of Geophysical Research: Atmospheres* 116.
38. Lachniet MS, *et al.* (2004) A 1500-year El Nino/Southern Oscillation and rainfall history for the Isthmus of Panama from speleothem calcite. *J Geophys Res-Atmos* 109.
39. Wahl D, Byrne R, & Anderson L (2014) An 8700 year paleoclimate reconstruction from the southern Maya lowlands. *Quaternary Sci Rev* 103:19-25.
40. Stahle D, *et al.* (2012) Pacific and Atlantic influences on Mesoamerican climate over the past millennium. *Clim Dynam* 39(6):1431-1446.
41. Giddings L & Soto M (2003) Rhythms of precipitation in the Yucatan Peninsula. *The Lowland Maya: Three Millennia at the Human-wildland Interface,* eds Fedick S, Allen M and Jiminez-Osornio J. (Haworth Press, Binghamton):77-90.
42. Pavia EG, Graef F, & Reyes J (2006) PDO-ENSO effects in the climate of Mexico. *J Climate* 19(24):6433-6438.
43. Mendoza B, García-Acosta V, Velasco V, Jáuregui E, & Díaz-Sandoval R (2007) Frequency and duration of historical droughts from the 16th to the 19th centuries in the Mexican Maya lands, Yucatan Peninsula. *Climatic Change* 83(1-2):151-168.
44. Medina-Elizalde M & Rohling EJ (2012) Collapse of Classic Maya Civilization Related to Modest Reduction in Precipitation. *Science* 335(6071):956-959.
45. Moy CM, Seltzer GO, Rodbell DT, & Anderson DM (2002) Variability of El Nino/Southern Oscillation activity at millennial timescales during the Holocene epoch. *Nature* 420(6912):162-165.
46. Hansen RD (2001) The First Cities: The Beginnings of Urbanization and State Formation in the Maya Lowlands. *Maya: Divine Kings of the Rainforest*, ed Grube N (Konneman Press, Verlag, Germany), pp 50-65.
47. Estrada-Belli F (2010) *The First Maya Civilization: Ritual and Power Before the Classic Period* (Routledge, London).
48. Hansen RD (2005) Perspectives on Olmec-Maya Interaction in the Middle Formative Period. *New Perspectives on Formative Mesoamerican Cultures*, ed Powis TG (British Archaeological Reports, Oxford), pp 51-72.
49. Stuart D (2000) Teotihuacan and Tollan in Classic Maya History. *Mesoamerica's Classic Heritage: From Teotihuacan to the Aztecs*, eds Carrasco D, Jones L, & Sessions S (University of Colorado Press, Boulder), pp 465-514.
50. Scarborough VL, *et al.* (2012) Water and sustainable land use at the ancient tropical city of Tikal, Guatemala. *Proceedings of the National Academy of Sciences* 109(31):12408-12413.
51. Martin S & Grube N (1995) Maya superstates. *Archaeology* 48(6):41-46.
52. Martin S & Grube N (2008) *Chronicle of the Maya Kings and Queens* (Thames and Hudson, London).

53. Webster DL (2002) *The Fall of the Ancient Maya: Solving the Mystery of the Maya Collapse* (Thames and Hudson, New York).
54. Demarest AA, Rice PM, & Rice DS (2004) The Terminal Classic in the Maya Lowlands: Assessing Collapses, Terminations, and Aftermaths. *The Terminal Classic in the Maya Lowlands: Collapse, Transition, and Transformation*, (University Press of Colorado, Boulder), pp 545–572.
55. Dunning NP & Beach T (2011) Farms and forests: Spatial and temporal perspectives on ancient Maya landscapes. *Landscapes and societies*, eds Martini IP and Chesworth W (Springer, Dordrecht), pp 369-389.
56. Rice DS & Rice PM (1990) Population size and population change in the central Peten lakes region, Guatemala. *Precolumbian population history in the Maya lowlands*, eds Culbert TP & Rice DS (University of New Mexico Press, Albuquerque), pp 123-148.
57. Turner II BL (1990) Population Reconstruction of the Central Maya Lowlands: 1000 B.C. to A.D. 1500. *Precolumbian population history in the Maya lowlands*, eds Culbert TP & Rice DS (University of New Mexico Press, Albuquerque), pp 301-324.
58. Dunning NP*, et al.* (2002) Arising from the bajos: The evolution of a neotropical landscape and the rise of Maya civilization. *Annals of the Association of American Geographers* 92(2):267-283.
59. Luzzadder-Beach S, Beach TP, & Dunning NP (2012) Wetland fields as mirrors of drought and the Maya abandonment. *Proceedings of the National Academy of Sciences* 109(10):3646-3651.
60. Eglinton TI, Aluwihare LI, Bauer JE, Druffel ERM, & McNichol AP (1996) Gas chromatographic isolation of individual compounds from complex matrices for radiocarbon dating. *Analytical Chemistry* 68(5):904-912.
61. Galy V & Eglinton T (2011) Protracted storage of biospheric carbon in the Ganges-Brahmaputra basin. *Nat Geosci* 4(12):843-847.
62. Blaauw M (2010) Methods and code for 'classical' age-modelling of radiocarbon sequences. *Quat Geochronol* 5(5):512-518.
63. Reimer PJ*, et al.* (2013) IntCal13 and Marine13 radiocarbon age calibration curves 0–50,000 years cal BP. *Radiocarbon* 55(4):1869-1887.
64. New M, Lister D, Hulme M, & Makin I (2002) A high-resolution data set of surface climate over global land areas. *Climate Research* 21(1):1-25.

Figure Legends

Figure 1 Map of the Maya Lowlands indicating the distribution of annual precipitation (64) and the location of paleoclimate archives. The locations of modern lake sediment and soil samples (Fig. 2) are indicated.

Figure 2 Scatter plot showing the negative relationship between annual precipitation and $\delta D_{wax\text{-}corr}$ measured in modern lake sediment and soil samples (Fig. 1). Results from Lake Chichancanab (CH) and Salpeten (SP) are indicated. The black line indicates a linear regression fit to these data, with regression statistics reported at the bottom of the plot. Large squares indicate mean values for each sampling region, with error bars indicating standard error of the mean in both $\delta D_{wax\text{-}corr}$ and annual precipitation. The black error bar indicates the 1σ error for $\delta D_{wax\text{-}corr}$ values (SI Text). Original δD_{wax} data from Ref. 17.

Figure 3 Plant-wax (green; left) and terrigenous-macrofossil (red; right) age-depth models for (A) Lake Chichancanab and (B) Lake Salpeten. The age probability density of individual radiocarbon analyses is shown. The black lines indicate the 'best' age model based on the weighted-mean of 1000 age model iterations (62). Colored envelopes indicate 95% confidence intervals.

Figure 4 (**A**) $\delta D_{wax\text{-}corr}$ records from Lakes Chichancanab and Salpeten, fit with a smoothing spline (thicker lines) to highlight centennial-scale trends. Colored envelopes indicate 1σ error in $\delta D_{wax\text{-}corr}$ values (±7‰) applied to the smoothing spline fits. Horizontal bands indicate the mean $\delta D_{wax\text{-}corr}$ values for lake surface sediments and soils from three regions within the Maya Lowlands with different mean annual precipitation (Fig. 2); the width of the bands indicates the standard error of regional mean values. (**B**) $\delta^{18}O$ records from two speleothems from the northern (Chaac) and southern (Yok I)

Maya lowlands (8, 9) (Fig. 1), plotted on a common scale to highlight differences in the range and amplitude of $\delta^{18}O$ variability for these two records.

Figure 5 Record of the difference in δD_{wax} ($\Delta\delta D_{wax}$) between Lake Chichancanab and Lake Salpeten, indicating changes in the precipitation gradient between the northern and southern Maya Lowlands. $\Delta\delta D_{wax}$ is calculated as the difference between smoothing spline curves fit to isotopic data from each lake core (Fig. 3). The grey envelope indicates the propagated 1σ error for $\Delta\delta D_{wax}$ (±10‰). Modern $\Delta\delta D_{wax}$ (Fig. 2) is indicated by the dashed line.

Figure 6 Coupled plant-wax isotope records of hydroclimate and land-use change from (**A**) Lake Chichancanab and (**B**) Lake Salpeten, alongside (**C**) estimates of population in the Lake Salpeten catchment (56) and population density in the central portion of the southern Maya Lowlands (57). $\delta D_{wax\text{-}corr}$ and $\delta^{13}C_{wax}$ records in (**A**) and (**B**) are fit to a smoothing spline (thicker lines) to highlight centennial-scale trends. Colored envelopes indicate 1σ error applied to the smoothing spline fits for $\delta D_{wax\text{-}corr}$ (±7‰) and $\delta^{13}C_{wax}$ (±0.5‰). Estimates of % C_4 plants are discussed in the SI Text.

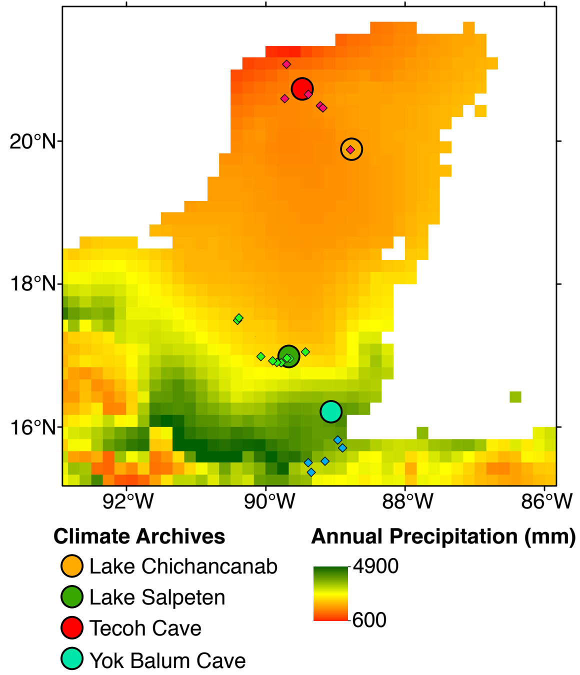
20°N
18°N
16°N
92°W
90°W
88°W
86°W
Climate Archives
Lake Chichancanab
Lake Salpeten
Tecoh Cave
Yok Balum Cave
Annual Precipitation (mm)
4900
600

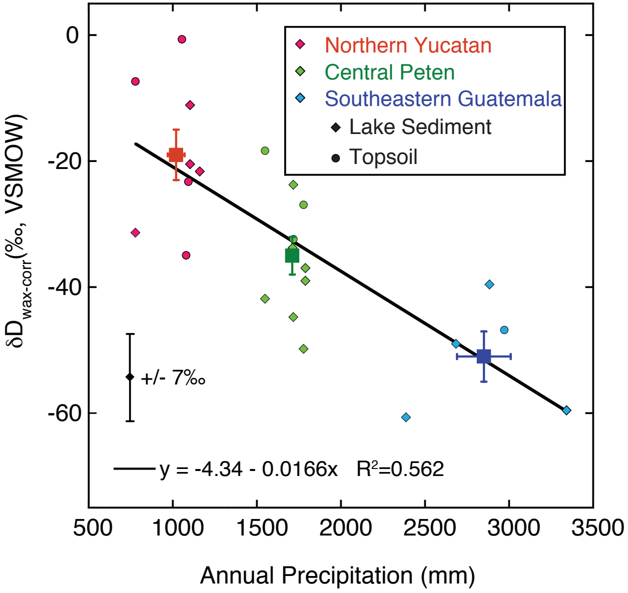

Northern Yucatan
Central Peten
Southeastern Guatemala
Lake Sediment
Topsoil
+/- 7‰
y = -4.34 - 0.0166x R²=0.562
0
-20
-40
-60
500
1000
1500
2000
2500
3000
3500
Annual Precipitation (mm)
δD wax-corr (‰, VSMOW)

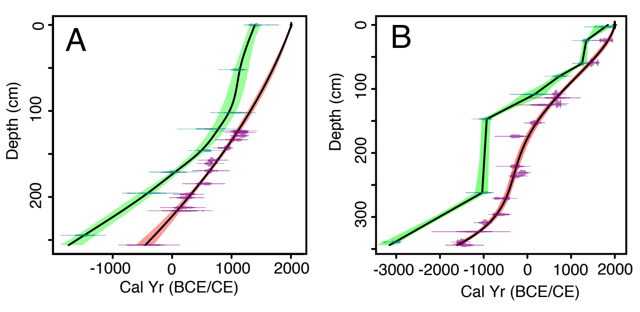

A
0
100
200
Depth (cm)
-1000
0
1000
2000
Cal Yr (BCE/CE)
B
0
100
200
300
Depth (cm)
-3000
-2000
-1000
0
1000
2000
Cal Yr (BCE/CE)

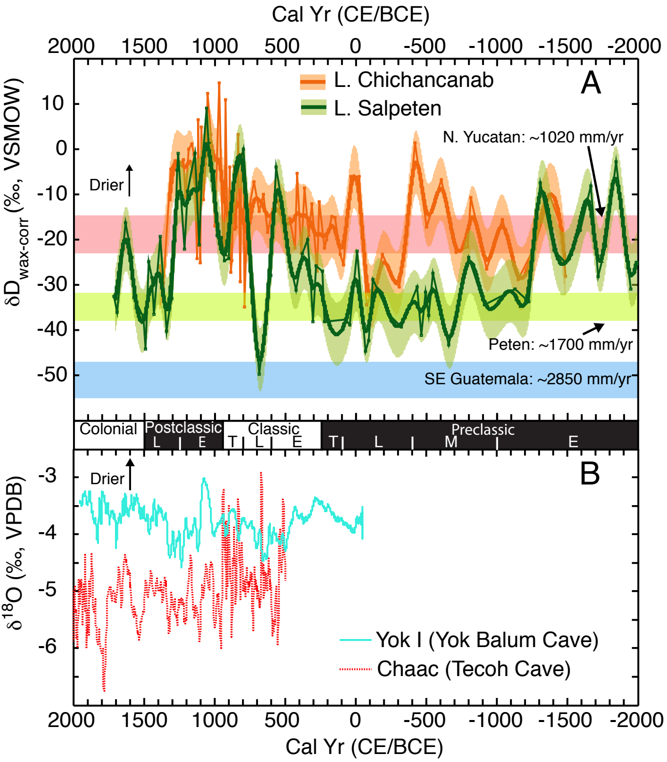
Cal Yr (CE/BCE)
2000
1500
1000
500
0
-500
-1000
-1500
-2000
A
L. Chichancanab
L. Salpeten
N. Yucatan: ~1020 mm/yr
Peten: ~1700 mm/yr
SE Guatemala: ~2850 mm/yr
Drier
δD wax-corr (‰, VSMOW)
10
0
-10
-20
-30
-40
-50
Colonial
Postclassic
L
E
Classic
T
L
E
Preclassic
T
L
M
E
B
Drier
δ18O (‰, VPDB)
-3
-4
-5
-6
Yok I (Yok Balum Cave)
Chaac (Tecoh Cave)
2000
1500
1000
500
0
-500
-1000
-1500
-2000
Cal Yr (CE/BCE)

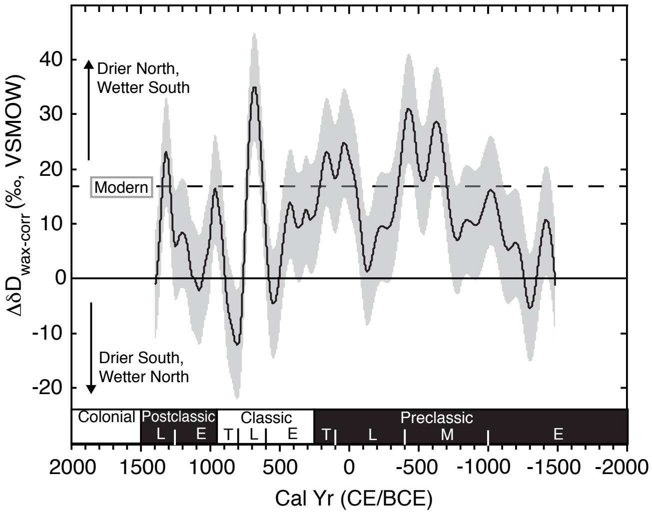

40
30
20
10
0
-10
-20
$\Delta\delta D_{wax\text{-}corr}$ (‰, VSMOW)
Drier North, Wetter South
Modern
Drier South, Wetter North
Colonial
Postclassic
L
E
Classic
T
L
E
Preclassic
T
L
M
E
2000
1500
1000
500
0
-500
-1000
-1500
-2000
Cal Yr (CE/BCE)

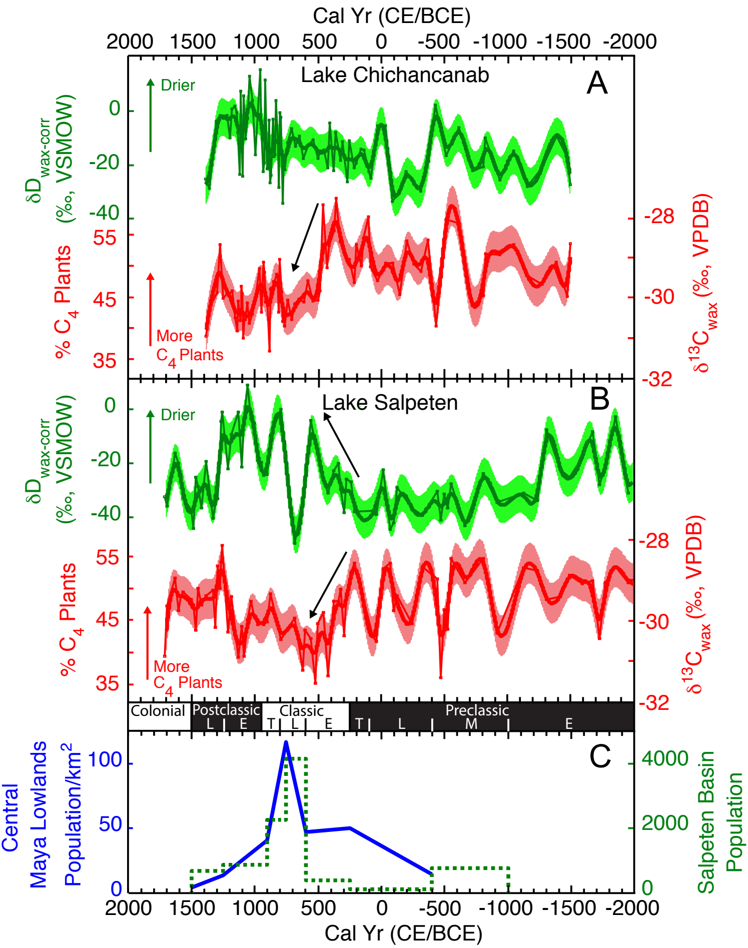
Cal Yr (CE/BCE)
2000
1500
1000
500
0
-500
-1000
-1500
-2000
Lake Chichancanab
A
Drier
δD wax-corr (‰, VSMOW)
0
-20
-40
55
45
35
% C4 Plants
More C4 Plants
-28
-30
-32
δ13C wax (‰, VPDB)
B
Lake Salpeten
Colonial
Postclassic
L
E
Classic
T
L
E
Preclassic
T
L
M
E
C
Central Maya Lowlands Population/km2
100
50
0
4000
2000
0
Salpeten Basin Population
Cal Yr (CE/BCE)

Drought, agricultural adaptation and sociopolitical collapse in the Maya Lowlands

Supplemental Text

Peter M. J. Douglas[1*†], Mark Pagani[1], Marcello A. Canuto[2], Mark Brenner[3], David A. Hodell[4], Timothy I. Eglinton[5,6], Jason H. Curtis[3]

For submission to Proceedings of the National Academy of Sciences

[1]Department of Geology and Geophysics, Yale University, New Haven, CT, USA

[2]Middle American Research Institute, Tulane University, New Orleans, LA, USA

[3]Department of Geological Sciences & Land Use and Environmental Change Institute, University of Florida, Gainesville, FL, USA

[4]Godwin Laboratory for Paleoclimate Research, Department of Earth Sciences, Cambridge University, Cambridge, UK

[5]Department of Marine Chemistry and Geochemistry, Woods Hole Oceanographic Institution, Woods Hole, MA, USA

[6]Geological Institute, ETH Zurich, Zurich, Switzerland

[*]Corresponding Author: pdouglas@caltech.edu

[†]Now at Division of Geological and Planetary Sciences, California Institute of Technology, Pasadena, CA, USA

Application of multiple homolog mean isotope values

In most lake sediment samples, there are multiple plant-wax homologs, i.e. plant waxes with different numbers of carbon atoms. Some studies have suggested that different plant taxa produce these plant waxes in different abundances (1, 2), but systematic taxonomic patterns are not well defined (3) and there is no consensus as to which homolog is the best indicator of hydroclimate change (δD_{wax}) or vegetation change ($\delta^{13}C_{wax}$).

In sediments from both Lakes Chichancanab and Salpeten, we observe substantial inter-homolog variability in both δD and $\delta^{13}C$. In both cases, the C_{28} homolog is the most D-enriched, C_{26} is most D-depleted, and C_{30} typically has intermediate values (Tables S2 and S3). At both lakes the C_{26} homolog is also typically the most ^{13}C-enriched, while differences between the C_{30} and C_{28} homologs in terms of $\delta^{13}C$ values are less consistent between the two lakes (Tables S2 and S3). Inter-homolog isotopic variability is evident in *n*-alkanoic acids from some plant extracts, but there are no clear patterns between plant taxa (4, 5). We suggest that the observed differences likely arise because of differences in the plant sources of these molecules. For instance, the high $\delta^{13}C$ values of the C_{26} *n*-alkanoic acid homolog suggests it is likely to have a relatively large source from C_4 grasses, whereas the C_{28} and C_{30} homologs likely have a larger source from C_3 flora.

In this study we focused on the mean δD and $\delta^{13}C$ values of the C_{26}, C_{28}, and C_{30} homologs for two reasons. First, because of sample-size limitations, our plant wax radiocarbon analyses were conducted on combined samples of the C_{26}, C_{28}, C_{30} and C_{32} homologs. There may be small differences in the ages of these individual homologs, and therefore it is appropriate to apply a mean stable isotope value when using these ages to understand the chronology of plant-wax stable isotope records. The C_{32} homolog was not sufficiently abundant for accurate stable isotope measurement in many samples, and is not included in mean δD_{wax} and $\delta^{13}C_{wax}$ values. This homolog, however, represents a very small fraction of the compound-specific radiocarbon samples (typically less than 5%), and probably does not influence the age-depth models significantly.

Second, different *n*-alkanoic acid homologs likely vary in their dominant plant sources, which potentially differ in their D/H response to hydroclimate change. Because there is no good rationale for selecting a single homolog as the best indicator of climate or vegetation change, the mean δD and $\delta^{13}C$ value of these homologs provides the most general indicator of past environmental change. Analyses of soils and lake surface sediments from southeastern Mexico and Guatemala indicate that mean δD_{wax} values are significantly correlated with climate variables, in many cases to a greater degree than δD values of individual homologs (6).

In this study we did not analyze abundance-weighted mean isotope values because there is substantial temporal variability in the relative abundance of the C_{26}, C_{28} and C_{30} homologs in these two cores. Because these homologs display large differences in their δD values, an abundance-weighted mean δD_{wax} record could be biased by variability in homolog relative abundance. In contrast, the unweighted mean value is not affected by homolog relative abundance. For consistency, we also applied unweighted mean $\delta^{13}C_{wax}$ records. Whereas the isotopic values of individual homologs are offset from one another, they display similar temporal patterns that are consistent with the evidence for climatic and vegetation changes inferred from the mean δD_{wax} and $\delta^{13}C_{wax}$ values.

Accounting for differences in δD_{wax} between plant groups

In addition to hydrological variables, δD_{wax} values can be influenced by differences in hydrogen isotope fractionation between different plant groups, with lower δD_{wax} in grasses than trees and shrubs from the same environment (5, 7), and it is possible that vegetation change can bias the δD_{wax} record of climatic change (6). A recent study (8) proposed a method for applying $\delta^{13}C_{wax}$ data to correct δD_{wax} records for vegetation change in tropical environments dominated by C_3 trees and shrubs and C_4 grasses. This method applies ε_a (the apparent hydrogen isotope fractionation between plant-source water and plant waxes) values measured in C_3 trees and shrubs and C_4 grasses, as well as end-member $\delta^{13}C_{wax}$ values for these two groups, to develop a vegetation-corrected δD_{wax} ($\delta D_{wax\text{-}corr}$) value, using the following equations:

$$f_{c4} = \frac{\delta^{13}C_{wax} - \delta^{13}C_{c3}}{\delta^{13}C_{c4} - \delta^{13}C_{c3}} \quad (3)$$

$$\varepsilon_a = f_{c4}(\varepsilon_{c4}) + (1 - f_{c4})(\varepsilon_{c3}) \quad (4)$$

$$\delta D_{wax-corr} = \left[\frac{\delta D_{wax} + 1000}{\left(\frac{\varepsilon_a}{1000}\right) + 1}\right] - 1000 \quad (5)$$

where f_{c4} is the estimated proportion of plant waxes derived from C_4 plants, $\delta^{13}C_{c3}$ and $\delta^{13}C_{c3}$ are end-member $\delta^{13}C_{wax}$ values for C_3 trees and shrubs and C_4 grasses respectively, and ε_{C3} and ε_{C4} are end-member apparent D/H fractionation factors for C_3 trees and shrubs and C_4 grasses, respectively.

We slightly modified the calculations of Ref. 8 to reflect that we analyze *n*-alkanoic acids as opposed to *n*-alkanes. To account for this difference we applied $\delta^{13}C_{c3}$

(-37.1±0.3 ‰), $\delta^{13}C_{c4}$ (-21.3±0.7 ‰), ε_{C3} (-94±4 ‰) and ε_{C4} (-122±4 ‰) values based on measurements of *n*-alkanoic acids in C_3 trees and C_4 grasses from East Asia (5), the only study that has compared *n*-alkanoic acid isotope values in C_3 and C_4 plants grown with water of known isotopic composition. We calculated these end-member values as the mean of the C_{26}, C_{28}, and C_{30} homologs in that study. The listed errors are 1σ standard error of the mean. We calculated a combined error for $\delta D_{wax\text{-}corr}$ values of ±7‰ using a Monte Carlo method in Matlab® that incorporated errors for the end-member values listed above, as well as analytical error for δD_{wax} (5‰) and $\delta^{13}C_{wax}$ (0.5‰). The combined error for $\delta D_{wax\text{-}corr}$ is insensitive to δD_{wax} and $\delta^{13}C_{wax}$ values.

$\delta D_{wax\text{-}corr}$ values roughly approximate the δD composition of plant water, although further testing is required to assess how closely they approximate this value. Regardless, $\delta D_{wax\text{-}corr}$ values provide an indication of δD_{wax} variability that accounts for the influence of vegetation change. This technique is only applicable in environments where C_3 trees and shrubs and C_4 grasses are the dominant plant groups, and C_3 grasses and CAM plants are not abundant, as is the case in many low-elevation tropical regions with sub-arid to humid climates, including the Maya lowlands (9).

Applying the vegetation correction described above to the Lake Chichancanab and Lake Salpeten sediment cores, although shifting the overall δD value, does not produce an appreciably different record of climate variability (Fig. S1). This is because of the relatively modest degree of $\delta^{13}C_{wax}$ variability in these cores (<4‰), which indicates shifts in the relative abundance of C_3 and C_4 plants on the order of 20-30%, combined with large δD_{wax} variability (40-50‰).

$\delta^{13}C_{wax}$ as a recorder of Ancient Maya Land Use

The $\delta^{13}C$ of plant waxes is strongly determined by the carbon isotope composition of bulk plant tissue (1, 2, 5). In the Maya Lowlands, where the dominant natural vegetation is C_3 angiosperm forest, but where there are large amounts of C_4 grasses (9), especially under circumstances of human disturbance, the relative proportion of C_3 to C_4 plants is the dominant control on $\delta^{13}C_{wax}$ values in lake sediments (10). $\delta^{13}C_{wax}$ has similarly been applied as a robust indicator of the relative abundance of C_3 and C_4 plants in other tropical locations (11, 12)

In many natural settings the relative abundance of C_4 grasses is largely controlled by climate, because C_4 plants have a competitive advantage over trees and shrubs under hot, dry conditions. In fact, glacial-to-interglacial $\delta^{13}C_{wax}$ from a number of locations, including the Maya lowlands, have shown a strong dependence on climate (10, 11). Under ancient Maya land-use regimes, however, climatic controls on C_3/C_4 vegetation dynamics are likely to have been diminished. The ancient Maya cleared large areas of C_3 deciduous and evergreen tropical forest, which led to a large increase in the abundance of C_4 grasses and other disturbance taxa (13, 14). Most palynological studies in the Maya Lowlands have found that human land use, as opposed to climate change, was the dominant driver of vegetation cover change during the late Holocene (13, 15). Furthermore, the staple crop of the ancient Maya was maize, a C_4 grass, and ancient agricultural settings in the Maya lowlands exhibit strong $\delta^{13}C$ enrichment of soil organic carbon (16, 17). Therefore, the relative abundance of C_4 plants, inferred from $\delta^{13}C_{wax}$ measurements, is interpreted primarily as an indicator of ancient Maya land use.

The transport pathways for plant waxes from terrestrial ecosystems to lake sediment are not well constrained. Analyses of δD_{wax} and plant-wax radiocarbon ages ($\Delta^{14}C_{wax}$) in Lake Chichancanab sediments and catchment soils (18), however, indicate that in karst regions of the Maya Lowlands, they are primarily transported from catchment soils. The relatively old ^{14}C ages of plant waxes in lake surface sediments from the Maya Lowlands specifically argue against significant atmospheric input from aerosols (18). This means that sedimentary plant waxes are largely derived from within the lake catchment, and that $\delta^{13}C_{wax}$ values provide a local, catchment-integrated record of vegetation change. This is an important consideration in the context of the Maya Lowlands, where human land use led to high spatial variability in vegetation patterns (19, 20).

The ancient Maya practiced a wide range of land-use strategies, including swidden agriculture, terraced upland agriculture, wetland agriculture, agroforestry, and garden orchards (19-22). Abundances of C_4 plants in the Lake Chichancanab and Lake Salpeten sediment cores were likely controlled by the spatial coverage of upland agriculture within the lake catchments. These two catchments do not contain sizeable wetlands aside from the lakes themselves, and are therefore unlikely to have captured large amounts of plant waxes originating from wetland agricultural sites. Changes in the amount of land employed for upland staple crop agriculture, which typically involves the burning or clearing of forests and their replacement with largely C_4 crops (19, 20), would probably account for the strongest signal of relative abundance of C_4 plants. Other land uses that emphasize C_3 plants, such as agroforestry or orchards (23, 24), would be less likely to affect the $\delta^{13}C_{wax}$ signal with respect to natural vegetation.

Archaeological and sedimentological data both indicate a much larger human presence at Lake Salpeten than Lake Chichancanab, both in terms of the number of ancient residential structures surveyed (25) as well as evidence for major anthropogenic soil erosion in the Lake Salpeten sediments (26), which is not present in Lake Chichancanab sediments (27). The presence of *Zea* pollen in a low-resolution palynological record from Lake Chichancanab, however, indicates maize agriculture did occur in its catchment (15). The similar $\delta^{13}C_{wax}$ records between the two catchments suggest that human land-use effects on the abundance of C_4 plants were similar between the two catchments, despite the evidence for larger populations surrounding Lake Salpeten. This pattern is consistent with extensive swidden agriculture conducted by low-density populations leading to enhanced C_4 plant growth in both catchments during the Preclassic Period.

The palynological record from Lake Salpeten (14) provides a valuable comparison with the $\delta^{13}C_{wax}$ record from this lake (Fig. S4), although the pollen record has relatively low temporal resolution. The pollen record from Lake Salpeten has been interpreted as indicating a large increase in disturbance taxa, including grasses and weeds associated with anthropogenic deforestation, beginning in the early Preclassic period and lasting through the Terminal Classic, with a return to dominance of tropical forest taxa during the Postclassic period (14, 26, 28). This interpretation is partially at odds with the $\delta^{13}C_{wax}$ record, which indicates a decrease in C_4 plants during the Early Classic period, much earlier than the decline in disturbance taxa pollen. When the disturbance taxa are disaggregated, however, it is apparent that *Poaceae* (grass) pollen, the family accounting for most C_4 plants in the region, began to decline in the Late Preclassic (Fig. S4B). Given the low resolution of the pollen data this decrease in *Poaceae* is consistent with evidence for decreasing C_4 plants in the Classic Period from the $\delta^{13}C_{wax}$ record. In contrast, other disturbance taxa such as *Asteraceae* and *Ambrosia,* which are dominantly C_3 plants, increased in abundance through the Classic period (Fig. S4C,D). One explanation for these patterns, consistent with both the $\delta^{13}C_{wax}$ record and population estimates, is that during the Classic period the predominant land use in the Lake Salpeten catchment shifted from low-population-density swidden agriculture, which promoted grasses, to higher-population-density residential land use that promoted the growth of C_3 disturbance flora including *Asteraceae* and *Ambrosia*.

Zea (maize) pollen is also present in Salpeten sediments in horizons spanning the late Preclassic to early Classic, including the period of minimum $\delta^{13}C_{wax}$ values (Fig. S4B). There are two key points in interpreting the presence of *Zea* pollen. First, *Zea* pollen is not abundant in the sediment core, and although its presence indicates maize agriculture, it does not provide strong evidence for the abundance of maize in the catchment (29). Second, *Zea* pollen grains have a relatively short transport distance (~200 m) (30, 31), and therefore primarily represent maize production close to the lake. We suggest that the continued presence of maize pollen in the lake sediments during the Classic period, concurrent with evidence for an overall decrease in C_4 plants in the lake catchment, suggests that maize agriculture did continue in the Salpeten basin, but at lower levels than occurred during the Preclassic. Maize cultivation in the catchment may have shifted from the hillslopes to the lakeshore during the Classic, a shift that could have enhanced the preservation of maize pollen in the lake sediments even as overall catchment C_4 plant abundance declined. This scenario would be consistent with the adoption of water conservative agriculture in the Classic period, as agriculture near the lakeshore would have been better able to access the perched aquifer that feeds the lake, than would crops grown on the catchment hillslopes.

Age-depth models for plant-wax stable isotope records

Sediments from both Lakes Chichancanab and Salpeten contain a large proportion of pre-aged plant waxes, as indicated by plant-wax ^{14}C ($^{14}C_{wax}$) ages that are significantly older than the age of sediment deposition based on ^{14}C dating of terrigenous macrofossils (Fig. 3). This age offset poses a complication for reconstructing past changes in plant-wax stable isotope values, because terrigenous-macrofossil-derived (TM) age-depth models do not correspond to the time that the plant waxes were synthesized and their stable isotope values were recorded.

We addressed this complication by applying plant-wax specific (PW) age-depth models that rely on compound specific radiocarbon ages, as discussed in the main text. There are only two brief intervals in the upper meter of the sediment core in which the 95% confidence intervals of the PW and TM age models overlap (Fig. 3). $^{14}C_{wax}$ ages in the Lake Salpeten core change by only 20 years between 262 and 147 cm depth, suggesting that the age of deposited plant waxes is essentially invariant across this stratigraphic interval, which was a time of very rapid sediment deposition (Figure 3). Applying the PW age model to $\delta D_{wax\text{-}corr}$ and $\delta^{13}C_{wax}$ data from this interval of the sediment core results in data with very high temporal resolution (Figure S2B) whose interpretation is relatively uncertain in the context of this study. We do not include these data in our analysis of $\delta D_{wax\text{-}corr}$ and $\delta^{13}C_{wax}$ records of past environmental change, which is focused on centennial-scale variability.

To assess the ability of the Lake Salpeten PW and TM age-depth models to accurately reflect the chronology of plant-wax stable isotope variability, we compared $\delta D_{wax\text{-}corr}$ records fit to both of these age models with $\delta^{18}O$ records from Lake Salpeten (28) and the nearby Yok I speleothem from Belize (32) (Fig. S2). The δD_{wax} record fit to the PW age model (Figure S2B) is in broad agreement with centennial climate variability evident in the Yok I speleothem $\delta^{18}O$ record (Figure S2C). In contrast, the δD_{wax} record fit to the TM age model (Figure S2A) is temporally offset from the Yok I speleothem $\delta^{18}O$ record.

The δD_{wax} record fit to the PW age model also records long-term trends towards wetter conditions from 3200 to 2200 years BP and towards drier conditions from 1800 to 1000 years BP that are apparent in the Lake Salpeten $\delta^{18}O$ record (Figure S2D). The $\delta D_{wax\text{-}corr}$ record fit to the TM age model, in contrast, records a trend towards wetter conditions from 2000 to 1200 years BP that does not agree with the Lake Salpeten $\delta^{18}O$ record. Although the Lake Salpeten $\delta^{18}O$ record has been interpreted to have been partially controlled by changes in runoff caused by anthropogenic deforestation and afforestation, it is likely that long-term trends in this record are in large part a consequence of changes in the ratio of evaporation to precipitation (28). In particular, the trend towards elevated $\delta^{18}O$ values beginning at ~200 CE precedes pollen evidence for afforestation by at least 500 years (28), suggesting that it primarily reflects climatic change.

Similar results are found for Lake Chichancanab, with the δD_{wax} record fit to the PW age model providing a better fit to regional proxy records for hydroclimate from the northern Maya Lowlands (18). We also conducted an inverse modeling exercise to determine which plant-wax age distributions provided the best fit between δD_{wax} and the 7500-year gastropod $\delta^{18}O$ record from Lake Chichancanab (27). The best correspondence between these two records is achieved with plant-wax age distributions in which the majority (>80%) of plant waxes are cycled on millennial time scales and the age variance of this millennially cycled pool of plant waxes is relatively small (< 200 years) (18). This age distribution is consistent with the PW age model and provides an accurate record of past δD_{wax} variability on millennial and centennial time scales.

Because of the lack of high-resolution, long-term (i.e. >3500 years) climate records from the southern Maya Lowlands, the inverse modeling approach applied at Lake Chichancanab is not feasible at Lake Salpeten. Nevertheless, the Lake Chichancanab and Lake Salpeten catchments are both characterized by karst hydrology, and plant-wax transport pathways and age distributions for the two lakes are probably similar. Furthermore, the presence of high-amplitude δD_{wax} variability in records from both lakes (18) (Fig. S2B) provides a strong argument against significant mixing of plant waxes of different ages and further supports the application of PW age models.

References

1. Rommerskirchen F, Plader A, Eglinton G, Chikaraishi Y, & Rullkotter J (2006) Chemotaxonomic significance of distribution and stable carbon isotopic composition of long-chain alkanes and alkan-1-ols in C-4 grass waxes. *Org Geochem* 37(10):1303-1332.
2. Vogts A, Moossen H, Rommerskirchen F, & Rullkotter J (2009) Distribution patterns and stable carbon isotopic composition of alkanes and alkan-1-ols from plant waxes of African rain forest and savanna C-3 species. *Org Geochem* 40(10):1037-1054.

3. Bush RT & McInerney FA (2013) Leaf wax *n*-alkane distributions in and across modern plants: Implications for paleoecology and chemotaxonomy. *Geochim Cosmochim Ac* 117:161-179.
4. Chikaraishi Y & Naraoka H (2007) $\delta^{13}C$ and δD relationships among three n-alkyl compound classes (n-alkanoic acid, n-alkane and n-alkanol) of terrestrial higher plants. *Org Geochem* 38(2):198-215.
5. Chikaraishi Y, Naraoka H, & Poulson SR (2004) Hydrogen and carbon isotopic fractionations of lipid biosynthesis among terrestrial (C3, C4 and CAM) and aquatic plants. *Phytochemistry* 65(10):1369-1381.
6. Douglas PMJ, Pagani M, Brenner M, Hodell DA, & Curtis JH (2012) Aridity and vegetation composition are important determinants of leaf-wax δD values in southeastern Mexico and Central America. *Geochim Cosmochim Ac* 97:24-45.
7. Sachse D*, et al.* (2012) Molecular paleohydrology: Interpreting the hydrogen-isotopic composition of lipid biomarkers from photosynthesizing organisms. *Annual Review of Earth and Planetary Sciences* 40:221-249.
8. Collins JA*, et al.* (2013) Estimating the hydrogen isotopic composition of past precipitation using leaf-waxes from western Africa. *Quaternary Sci Rev* 65:88-101.
9. Sage RF, Wedin DA, & Li M (1999) The biogeography of C4 photosynthesis: patterns and controlling factors. *C4 Plant Biology*, eds Sage RF & Monson RK (Academic Press, San Diego), pp 313-373.
10. Huang Y*, et al.* (2001) Climate change as the dominant control on glacial-interglacial variations in C-3 and C-4 plant abundance. *Science* 293(5535):1647-1651.
11. Hughen KA, Eglinton TI, Xu L, & Makou M (2004) Abrupt tropical vegetation response to rapid climate changes. *Science* 304(5679):1955-1959.
12. Huang YS, Dupont L, Sarnthein M, Hayes JM, & Eglinton G (2000) Mapping of C_4 plant input from North West Africa into North East Atlantic sediments. *Geochim Cosmochim Ac* 64(20):3505-3513.
13. Wahl D, Byrne R, Schreiner T, & Hansen R (2006) Holocene vegetation change in the northern Peten and its implications for Maya prehistory. *Quaternary Res* 65(3):380-389.
14. Leyden BW (1987) Man and Climate in the Maya Lowlands. *Quaternary Res* 28(3):407-417.
15. Leyden BW (2002) Pollen evidence for climatic variability and cultural disturbance in the Maya lowlands. *Ancient Mesoamerica* 13:85-101.
16. Beach T*, et al.* (2011) Carbon isotopic ratios of wetland and terrace soil sequences in the Maya Lowlands of Belize and Guatemala. *Catena* 85(2):109-118.
17. Webb EA*, et al.* (2007) Stable carbon isotope signature of ancient maize agriculture in the soils of Motul de San Jose, Guatemala. *Geoarchaeology* 22(3):291-312.
18. Douglas PM*, et al.* (2014) Pre-aged plant waxes in tropical lake sediments and their influence on the chronology of molecular paleoclimate proxy records. *Geochim Cosmochim Ac* 141: 346-364.

19. Turner B & Sabloff JA (2012) Classic Period collapse of the Central Maya Lowlands: Insights about human–environment relationships for sustainability. *Proceedings of the National Academy of Sciences* 109(35):13908-13914.
20. Dunning NP & Beach T (2011) Farms and forests: Spatial and temporal perspectives on ancient Maya landscapes. *Landscapes and societies*, eds Martini IP and Chesworth W (Springer, Dordrecht), pp 369-389.
21. Dunning NP*, et al.* (2002) Arising from the bajos: The evolution of a neotropical landscape and the rise of Maya civilization. *Annals of the Association of American Geographers* 92(2):267-283.
22. Turner II BL (1974) Prehistoric Intensive Agriculture in the Mayan Lowlands. *Science* 185:118-124.
23. Lentz DL & Hockaday B (2009) Tikal timbers and temples: Ancient Maya agroforestry and the end of time. *J Archaeol Sci* 36(7):1342-1353.
24. Ross NJ (2011) Modern tree species composition reflects ancient Maya "forest gardens" in northwest Belize. *Ecol Appl* 21(1):75-84.
25. Rice DS & Rice PM (1990) Population size and population change in the central Peten lakes region, Guatemala. *Precolumbian population history in the Maya lowlands*, eds Culbert TP & Rice DS (University of New Mexico Press, Albuquerque), pp 123-148.
26. Anselmetti FS, Hodell DA, Ariztegui D, Brenner M, & Rosenmeier MF (2007) Quantification of soil erosion rates related to ancient Maya deforestation. *Geology* 35(10):915-918.
27. Hodell DA, Curtis JH, & Brenner M (1995) Possible Role of Climate in the Collapse of Classic Maya Civilization. *Nature* 375(6530):391-394.
28. Rosenmeier MF, Hodell DA, Brenner M, Curtis JH, & Guilderson TP (2002) A 4000-year lacustrine record of environmental change in the southern Maya lowlands, Peten, Guatemala. *Quaternary Res* 57(2):183-190.
29. Taylor Z, Horn S, & Finkelstein D (2013) Maize pollen concentrations in Neotropical lake sediments as an indicator of the scale of prehistoric agriculture. *The Holocene* 23(1):78-84.
30. Luna V*, et al.* (2001) Maize pollen longevity and distance isolation requirements for effective pollen control. *Crop Science* 41(5):1551-1557.
31. Lane CS, Cummings KE, & Clark JJ (2010) Maize pollen deposition in modern lake sediments: A case study from Northeastern Wisconsin. *Rev Palaeobot Palyno* 159(3):177-187.
32. Kennett DJ*, et al.* (2012) Development and Disintegration of Maya Political Systems in Response to Climate Change. *Science* 338(6108):788-791.

Figure S1 Comparison of $\delta D_{wax-raw}$ and $\delta D_{wax-corr}$ records from Lake Salpeten and Lake Chichancanab. The mean values of the two records are aligned, and the axes are scaled to indicate the same range of variability. Error bars indicate the combined error for $\delta D_{wax-corr}$ values. The range of variability in the vegetation corrected data ($\delta D_{wax-corr}$) is not significantly different from the $\delta D_{wax-raw}$ data for the entirety of both records.

Figure S2 The Lake Salpeten $\delta D_{wax-corr}$ record fit to the A) TM age model and B) PW age model compared with hydroclimate proxy records from the southern Maya Lowlands. Horizontal lines indicate the mean value for each record. Colored vertical bars indicate periods of relatively wet (blue) and dry (orange) conditions as recorded by the Yok Speleothem $\delta^{18}O$ record (32) (C). Arrows indicate long-term climate trends inferred from the Lake Salpeten ostracod $\delta^{18}O$ record (28) (D).

Fig S3 Scatter plots showing relationships between $\delta D_{wax-corr}$ and (A) annual precipitation (P); (B) relative humidity; (C) Annual Potential Evapotranspiration (PET); and (D) the aridity index (AI, defined as P/PET); and relationships between between AI and P (E) and PET (F). The strongest determinant of $\delta D_{wax-corr}$ is annual precipitation. A similarly strong relationship is observed between $\delta D_{wax-corr}$ and AI. Most of the variance in AI at the sampling sites is explained by annual precipitation however (E), while much less is explained by potential evapotranspiration (F), further confirming that precipitation is more important than potential evapotranspiration in controlling spatial variability in $\delta D_{wax-corr}$.

Figure S4 Comparison of $\delta^{13}C_{wax}$ (**A**) and disturbance pollen records (**B, C, D, E**) (14) from Lake Salpeten. All pollen data are presented as percent of total pollen. Asterisks in (**B**) indicate the presence of maize (*Zea*) pollen. Pollen data are fit to the age-depth model of Ref. 26. The relative abundance of grass (*Poaceae*) pollen decrease beginning in the Late Preclassic, while *Asteraceae* and *Ambrosia* continue to increase through the Classic.

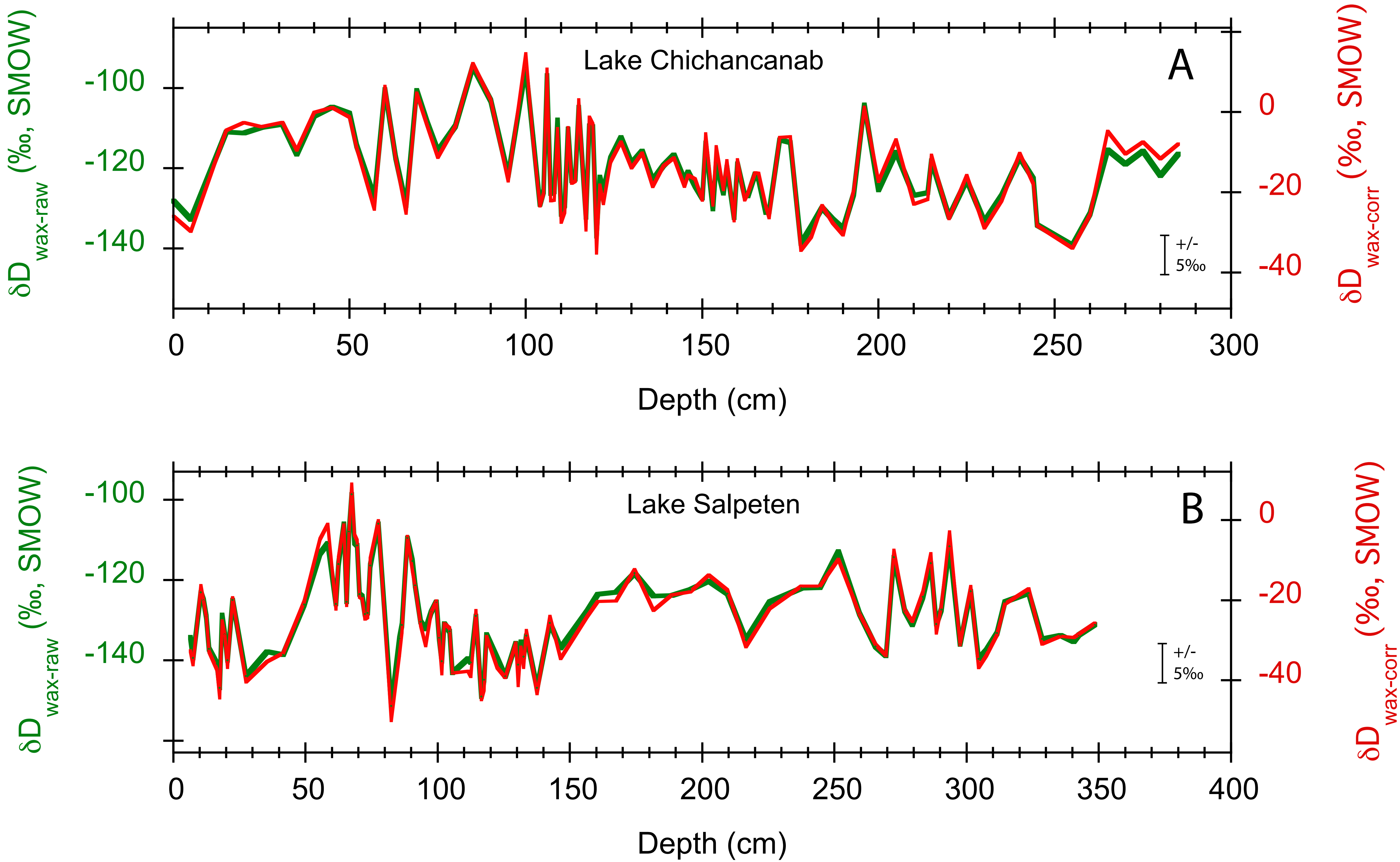

Lake Chichancanab
A
δDwax-raw (‰, SMOW)
-100
-120
-140
δDwax-corr (‰, SMOW)
0
-20
-40
+/- 5‰
0
50
100
150
200
250
300
Depth (cm)
Lake Salpeten
B
δDwax-raw (‰, SMOW)
-100
-120
-140
δDwax-corr (‰, SMOW)
0
-20
-40
+/- 5‰
0
50
100
150
200
250
300
350
400
Depth (cm)

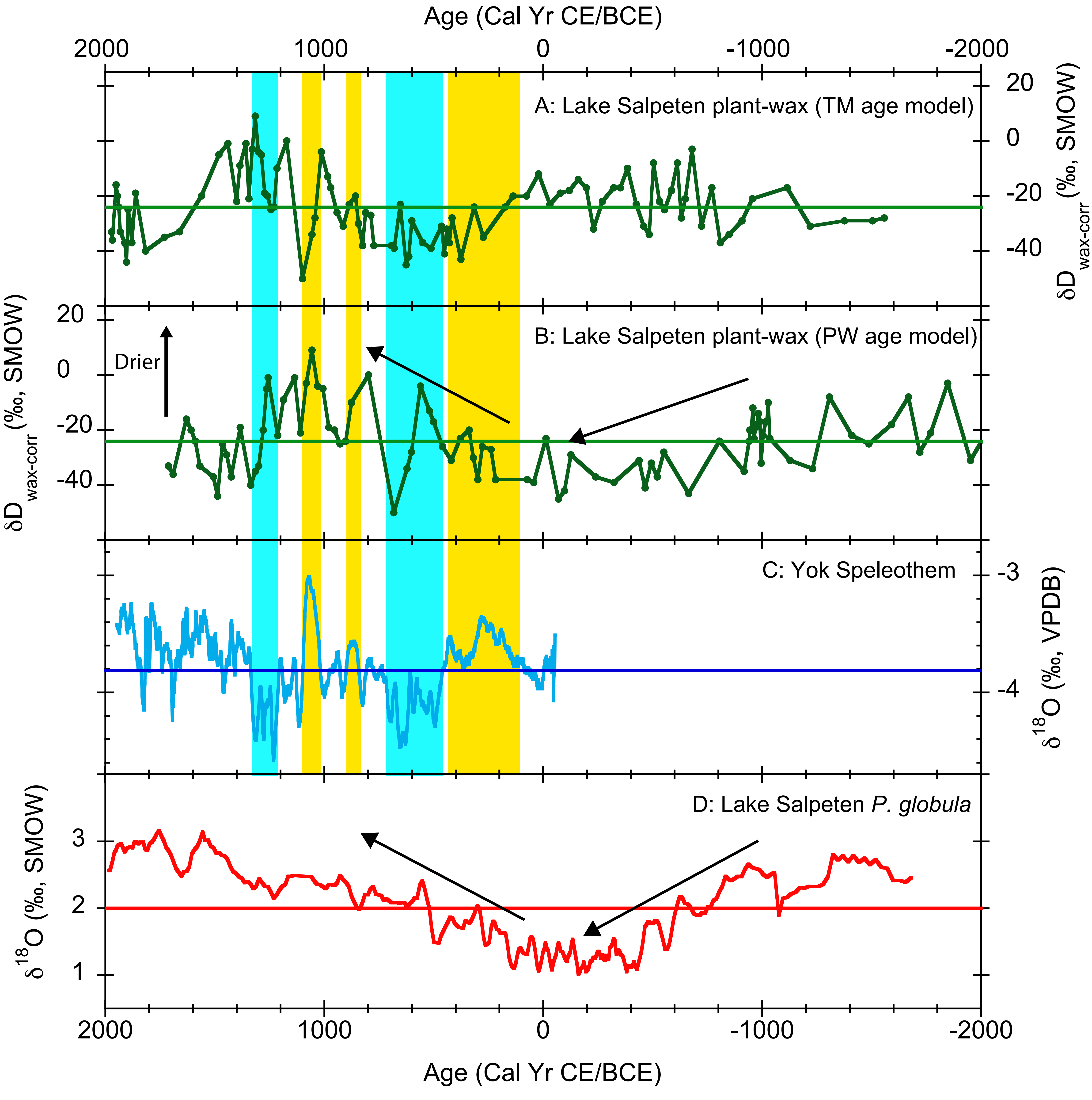

Age (Cal Yr CE/BCE)
2000
1000
0
-1000
-2000
A: Lake Salpeten plant-wax (TM age model)
20
0
-20
-40
δD wax-corr (‰, SMOW)
B: Lake Salpeten plant-wax (PW age model)
Drier
C: Yok Speleothem
-3
-4
δ18O (‰, VPDB)
D: Lake Salpeten P. globula
3
2
1
δ18O (‰, SMOW)

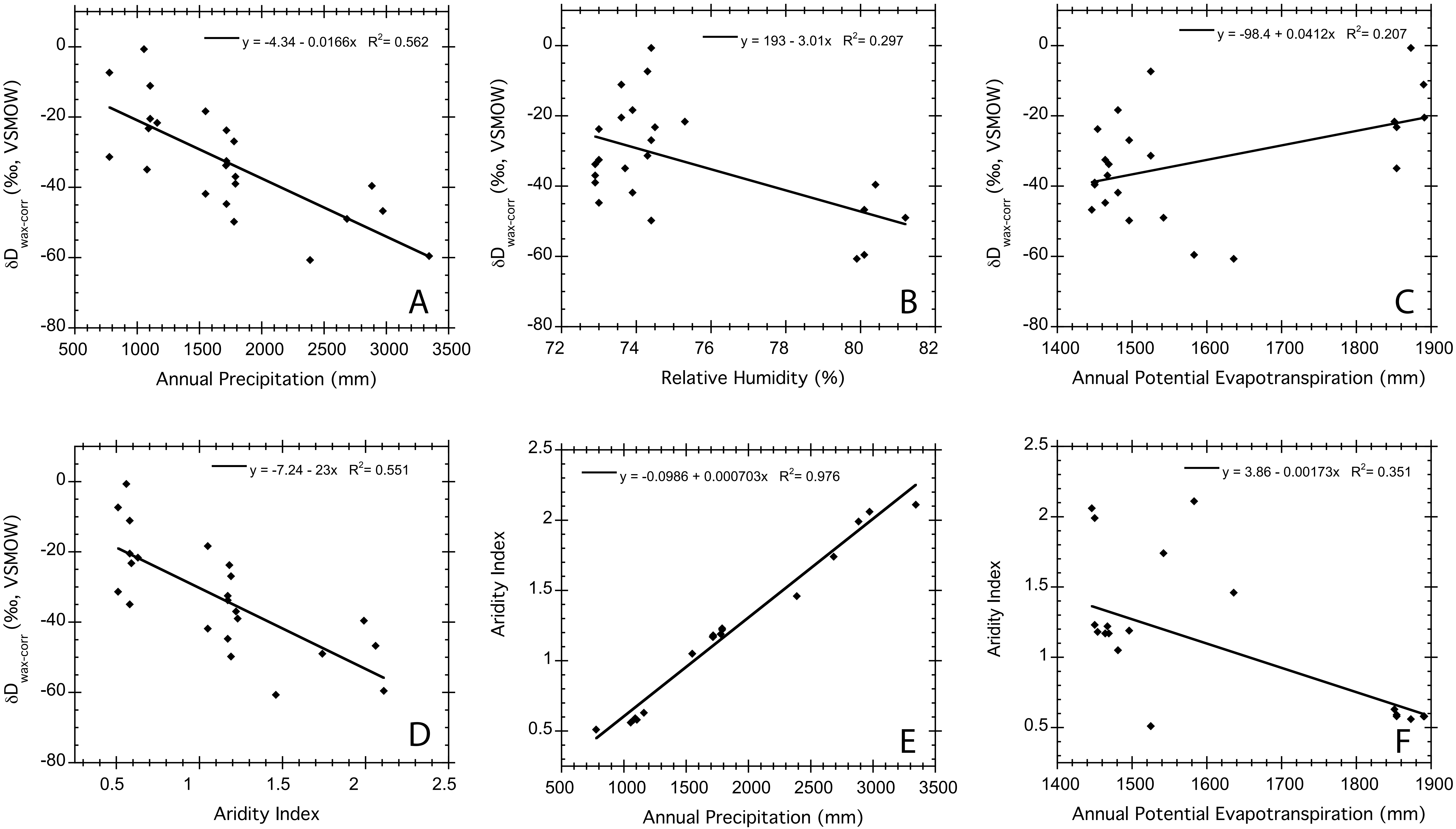

y = -4.34 - 0.0166x R2= 0.562
δDwax-corr (‰, VSMOW)
Annual Precipitation (mm)
A
y = 193 - 3.01x R2= 0.297
δDwax-corr (‰, VSMOW)
Relative Humidity (%)
B
y = -98.4 + 0.0412x R2= 0.207
δDwax-corr (‰, VSMOW)
Annual Potential Evapotranspiration (mm)
C
y = -7.24 - 23x R2= 0.551
δDwax-corr (‰, VSMOW)
Aridity Index
D
y = -0.0986 + 0.000703x R2= 0.976
Aridity Index
Annual Precipitation (mm)
E
y = 3.86 - 0.00173x R2= 0.351
Aridity Index
Annual Potential Evapotranspiration (mm)
F

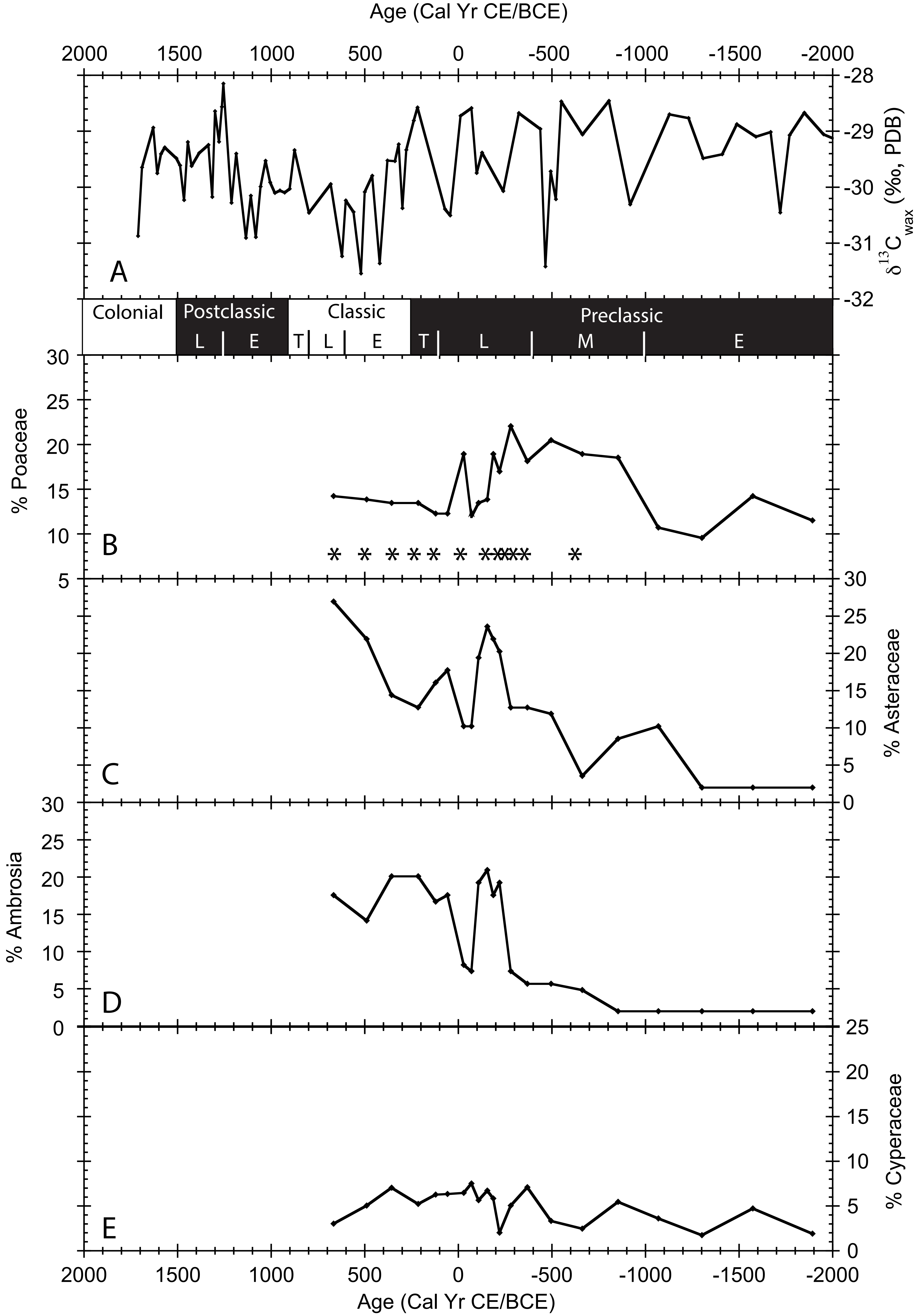

Age (Cal Yr CE/BCE)
2000
1500
1000
500
0
-500
-1000
-1500
-2000
-28
-29
-30
-31
-32
$\delta^{13}C_{wax}$ (‰, PDB)
A
Colonial
Postclassic
Classic
Preclassic
L
E
T
L
E
T
L
M
E
30
25
20
15
10
5
% Poaceae
B
% Asteraceae
C
0
% Ambrosia
D
% Cyperaceae
E
Age (Cal Yr CE/BCE)

Table S1: Lake Chichancanab Plant-wax Stable Isotope Data

Depth (cm)	TM Age 95% CI Lower	TM Age 'Best' (Yr BP)	TM Age 95% CI Upper	PW age 95% CI lower	PW Age 'Best' (Yr BP)	PW age 95% CI Upper	$\delta^{13}C$ C26 (‰)	$\delta^{13}C$ C28 (‰)	$\delta^{13}C$ C30 (‰)	$\delta^{13}C$ Mean (‰)	f_{c4}	δD C26 (‰)	δD C28 (‰)	δD C30 (‰)	δD Mean (‰)	ε_a (‰)	$\delta D_{wax\text{-}corr}$ (‰)
0	-75	-58	-49	433	559	654	-27.9	-32.1	-32.8	-30.9	0.39	-147	-104	-134	-128	-105	-26
5	-48	-31	-21	473	588	674	-27.9	-31.3	-31.5	-30.2	0.43	-154	-115	-129	-133	-106	-30
15	3	24	42	547	644	724	-27.4	-30.8	-31.5	-29.9	0.46	-133	-87	-113	-111	-107	-5
20	28	53	75	575	671	751	-26.4	-29.6	-30.1	-28.7	0.53	-127	-90	-116	-111	-109	-3
25	54	83	109	597	698	777	-27.8	-30.7	-31.6	-30.0	0.45	-129	-93	-108	-110	-107	-4
31	86	119	150	619	727	807	-27.5	-30.5	-31.6	-29.9	0.46	-127	-93	-108	-109	-107	-2
35	109	145	178	633	746	827	-27.0	-29.9	-30.7	-29.2	0.50	-128	-101	-121	-116	-108	-9
40	137	177	214	650	768	850	-27.2	-30.8	-31.5	-29.8	0.46	-124	-81	-115	-107	-107	0
45	167	210	250	667	788	871	-28.8	-31.1	-31.6	-30.5	0.42	-120	-87	-107	-105	-106	1
50	199	244	287	683	806	894	-27.6	-31.5	-33.4	-30.8	0.40	-123	-80	-116	-106	-105	-1
52	211	258	301	688	812	903	-27.6	-30.8	-31.9	-30.1	0.44	-133	-84	-125	-114	-106	-9
57	245	294	339	699	827	925	-27.8	-31.4	-32.5	-30.6	0.41	-140	-109	-133	-127	-106	-24
60	265	315	361	706	835	939	-28.1	-31.5	-31.2	-30.3	0.43	-118	-83	-100	-100	-106	6
63	286	337	384	713	842	952	-28.4	-31.5	-29.3	-29.7	0.47	-106	-119	-126	-117	-107	-11
66	307	359	408	721	849	965	-28.2	-30.0	-31.5	-29.9	0.45	-138	-114	-136	-129	-107	-25
69	328	382	431	729	857	977	-28.1	-31.7	-33.2	-31.0	0.39	-116	-74	-112	-101	-105	5
72	351	405	455	738	864	990	-28.6	-31.4	-31.6	-30.6	0.41	-122	-86	-118	-109	-106	-3
75	373	428	479	747	873	1005	-26.6	-29.9	-35.1	-30.5	0.41	-126	-90	-130	-116	-106	-11
80	411	467	519	763	888	1029	-27.9	-30.9	-31.6	-30.1	0.44	-125	-88	-115	-109	-106	-3
85	451	507	560	783	905	1056	-26.0	-30.0	-35.9	-30.6	0.41	-107	-51	-126	-95	-105	12
90	492	548	601	805	927	1084	-28.7	-31.6	-30.9	-30.4	0.42	-112	-74	-123	-103	-106	3
95	534	590	643	833	953	1114	-28.0	-30.4	-31.6	-30.0	0.45	-125	-118	-127	-124	-107	-17
100	577	633	685	865	985	1145	-27.6	-30.2	-30.0	-29.3	0.49	-105	-77	-103	-95	-108	15
102	594	650	702	880	999	1157	-28.7	-31.3	-31.1	-30.4	0.43	-126	-86	-124	-112	-106	-7

Table S1 cont: Lake Chichancanab Plant-wax Stable Isotope Data

Depth (cm)	TM Age 95% CI Lower	TM Age 'Best' (Yr BP)	TM Age 95% CI Upper	PW age 95% CI lower	PW Age 'Best' (Yr BP)	PW age 95% CI Upper	$\delta^{13}C$ C26 (‰)	$\delta^{13}C$ C28 (‰)	$\delta^{13}C$ C30 (‰)	$\delta^{13}C$ Mean (‰)	f_{c4}	δD C26 (‰)	δD C28 (‰)	δD C30 (‰)	δD Mean (‰)	ε_a (‰)	$\delta D_{wax-corr}$ (‰)
104	612	668	720	896	1015	1169	-28.5	-29.7	-29.1	-29.1	0.51	-140	-112	-135	-129	-108	-23
105	621	677	728	904	1023	1176	-28.3	-30.0	-29.8	-29.4	0.49	-140	-104	-133	-126	-108	-20
106	630	686	737	911	1031	1183	-28.4	-31.0	-30.9	-30.1	0.44	-111	-71	-109	-97	-106	11
107	639	694	746	920	1040	1189	-29.2	-30.8	-30.2	-30.1	0.45	-142	-106	-131	-126	-106	-22
108	649	703	755	929	1049	1196	-29.1	-30.9	-30.5	-30.2	0.44	-138	-105	-134	-126	-106	-22
109	658	712	763	938	1058	1203	-29.3	-31.7	-33.0	-31.3	0.37	-122	-82	-119	-108	-104	-4
110	667	721	772	948	1067	1209	-28.8	-30.5	-30.0	-29.8	0.46	-147	-110	-137	-131	-107	-27
111	676	730	781	957	1076	1217	-28.7	-30.8	-29.8	-29.8	0.46	-141	-106	-141	-129	-107	-25
112	686	739	790	966	1086	1224	-28.4	-31.1	-30.3	-29.9	0.45	-123	-92	-116	-110	-107	-4
113	695	748	799	975	1095	1231	-28.3	-30.3	-30.2	-29.6	0.47	-138	-96	-136	-123	-107	-18
114	705	757	808	984	1105	1239	-28.6	-30.2	-30.0	-29.6	0.47	-137	-97	-134	-123	-107	-17
115	714	767	817	994	1115	1246	-27.6	-30.0	-30.8	-29.4	0.49	-116	-77	-121	-105	-108	3
116	723	776	826	1004	1124	1254	-27.9	-29.9	-30.6	-29.5	0.48	-134	-95	-127	-119	-108	-12
117	733	785	834	1013	1134	1261	-29.5	-30.8	-30.8	-30.4	0.43	-142	-119	-135	-132	-106	-29
118	743	794	843	1023	1144	1269	-28.0	-30.4	-28.7	-29.0	0.51	-121	-89	-119	-109	-108	-1
119	752	803	853	1033	1154	1278	-28.4	-29.6	-31.6	-29.9	0.46	-117	-93	-118	-110	-107	-3
120	761	813	862	1044	1164	1287	-29.6	-30.9	-31.3	-30.6	0.41	-149	-126	-135	-137	-106	-35
121	771	822	871	1054	1174	1294	-27.3	-29.9	-34.1	-30.4	0.42	-125	-99	-143	-122	-106	-18
122	781	832	880	1065	1184	1303	-29.0	-31.1	-32.0	-30.7	0.40	-138	-114	-125	-126	-105	-23
124	800	850	898	1086	1203	1322	-28.2	-30.5	-31.5	-30.1	0.45	-128	-103	-122	-118	-106	-12
127	830	879	926	1119	1233	1352	-28.4	-30.9	-32.3	-30.5	0.42	-131	-102	-104	-112	-106	-7
130	860	908	954	1155	1264	1382	-28.1	-30.4	-32.0	-30.2	0.44	-133	-111	-113	-119	-106	-14
133	890	937	982	1191	1296	1414	-27.8	-30.5	-31.8	-30.0	0.45	-129	-100	-118	-116	-107	-10
136	921	967	1010	1230	1329	1448	-28.1	-30.4	-31.8	-30.1	0.44	-137	-114	-118	-123	-106	-19

Table S1 cont: Lake Chichancanab Plant-wax Stable Isotope Data

Depth (cm)	TM Age 95% CI Lower	TM Age 'Best' (Yr BP)	TM Age 95% CI Upper	PW age 95% CI lower	PW Age 'Best' (Yr BP)	PW age 95% CI Upper	$\delta^{13}C$ C26 (‰)	$\delta^{13}C$ C28 (‰)	$\delta^{13}C$ C30 (‰)	$\delta^{13}C$ Mean (‰)	f_{c4}	δD C26 (‰)	δD C28 (‰)	δD C30 (‰)	δD Mean (‰)	ε_a (‰)	$\delta D_{wax\text{-}corr}$ (‰)
139	952	996	1038	1271	1364	1484	-27.4	-30.6	-30.7	-29.6	0.48	-133	-106	-119	-119	-107	-13
142	983	1026	1067	1316	1402	1521	-27.9	-30.5	-31.8	-30.1	0.44	-134	-97	-118	-117	-106	-11
145	1014	1057	1096	1363	1443	1558	-28.4	-30.5	-31.2	-30.1	0.45	-140	-112	-118	-123	-106	-18
146	1025	1067	1106	1379	1457	1572	-27.5	-30.1	-31.9	-29.8	0.46	-138	-104	-121	-121	-107	-16
148	1046	1088	1126	1412	1487	1598	-26.5	-28.9	-29.6	-28.3	0.56	-134	-102	-136	-124	-110	-17
150	1067	1108	1146	1447	1518	1626	-26.9	-29.1	-31.8	-29.3	0.50	-138	-111	-134	-127	-108	-22
151	1078	1119	1156	1464	1535	1641	-26.7	-29.3	-30.1	-28.7	0.53	-128	-92	-120	-114	-109	-5
153	1100	1140	1176	1499	1568	1670	-26.3	-29.0	-29.7	-28.3	0.55	-150	-107	-133	-130	-110	-23
154	1110	1150	1186	1516	1585	1686	-26.2	-29.5	-26.9	-27.5	0.60	-131	-101	-125	-119	-111	-9
156	1132	1171	1206	1551	1620	1716	-26.5	-29.2	-30.1	-28.6	0.54	-143	-112	-124	-126	-109	-19
157	1143	1182	1217	1569	1637	1732	-26.5	-30.2	-29.4	-28.7	0.53	-135	-95	-128	-120	-109	-12
159	1165	1203	1238	1605	1674	1763	-27.5	-30.1	-29.6	-29.1	0.51	-153	-106	-138	-132	-108	-27
160	1176	1214	1248	1623	1692	1779	-26.8	-30.5	-29.8	-29.0	0.51	-131	-86	-139	-119	-108	-12
162	1198	1235	1269	1661	1729	1812	-28.2	-30.9	-29.9	-29.6	0.47	-144	-99	-137	-127	-107	-22
163	1209	1246	1280	1678	1748	1829	-25.6	-30.1	-30.4	-28.7	0.53	-141	-104	-136	-127	-109	-20
165	1230	1268	1301	1715	1785	1862	-25.7	-30.0	-31.9	-29.2	0.50	-139	-93	-132	-121	-108	-15
166	1241	1279	1312	1734	1804	1879	-26.1	-29.9	-29.6	-28.5	0.54	-138	-97	-133	-123	-109	-15
168	1264	1300	1334	1770	1842	1913	-25.9	-29.0	-29.1	-28.0	0.58	-146	-112	-135	-131	-110	-23
169	1275	1311	1345	1788	1861	1931	-27.4	-31.1	-30.1	-29.5	0.48	-139	-113	-141	-131	-107	-26
172	1308	1345	1379	1843	1918	1988	-25.9	-29.4	-33.5	-29.6	0.48	-128	-87	-124	-113	-107	-6
175	1341	1378	1413	1896	1974	2048	-26.5	-30.3	-30.5	-29.1	0.50	-129	-89	-122	-114	-108	-6
178	1374	1412	1448	1949	2030	2112	-27.1	-30.1	-30.2	-29.1	0.50	-157	-114	-146	-139	-108	-34
181	1408	1446	1484	2000	2086	2177	-28.9	-30.4	-30.4	-29.9	0.45	-151	-115	-138	-134	-107	-31
184	1441	1481	1521	2052	2143	2243	-27.0	-29.5	-29.2	-28.6	0.54	-146	-106	-137	-130	-109	-23

Table S1 cont: Lake Chichancanab Plant-wax Stable Isotope Data

Depth (cm)	TM Age 95% CI Lower	TM Age 'Best' (Yr BP)	TM Age 95% CI Upper	PW age 95% CI lower	PW Age 'Best' (Yr BP)	PW age 95% CI Upper	$\delta^{13}C$ C26 (‰)	$\delta^{13}C$ C28 (‰)	$\delta^{13}C$ C30 (‰)	$\delta^{13}C$ Mean (‰)	f_{c4}	δD C26 (‰)	δD C28 (‰)	δD C30 (‰)	δD Mean (‰)	ε_a (‰)	$\delta D_{wax-corr}$ (‰)
187	1474	1516	1558	2104	2199	2310	-27.2	-29.2	-31.1	-29.2	0.50	-139	-120	-139	-133	-108	-28
190	1507	1551	1596	2156	2256	2378	-27.5	-29.8	-30.8	-29.4	0.49	-148	-117	-141	-135	-108	-31
193	1541	1586	1635	2210	2314	2444	-26.9	-28.9	-29.9	-28.6	0.54	-135	-110	-134	-126	-109	-19
196	1574	1622	1674	2264	2373	2510	-27.2	-30.0	-34.9	-30.7	0.40	-108	-74	-130	-104	-105	1
200	1619	1670	1727	2338	2453	2597	-25.4	-28.9	-29.9	-28.1	0.57	-146	-105	-122	-124	-110	-17
205	1675	1731	1795	2436	2556	2704	-24.9	-28.6	-31.0	-28.2	0.57	-133	-91	-123	-116	-110	-7
210	1732	1793	1864	2537	2661	2810	-25.7	-31.1	-33.8	-30.2	0.44	-151	-113	-116	-127	-106	-23
214	1777	1843	1920	2619	2747	2893	-27.2	-30.6	-32.1	-30.0	0.45	-145	-109	-124	-126	-107	-22
215	1788	1855	1935	2640	2768	2914	-25.6	-30.4	-30.8	-28.9	0.52	-138	-100	-117	-118	-108	-11
220	1845	1919	2007	2744	2877	3018	-26.3	-30.0	-30.6	-28.9	0.52	-154	-107	-136	-132	-108	-27
225	1902	1983	2080	2848	2988	3122	-26.8	-29.4	-29.9	-28.7	0.53	-145	-106	-118	-123	-109	-16
230	1960	2048	2155	2950	3100	3229	-27.3	-29.9	-31.2	-29.5	0.48	-153	-121	-125	-133	-108	-29
235	2017	2114	2231	3052	3212	3340	-27.9	-30.0	-31.1	-29.7	0.47	-146	-118	-117	-127	-107	-22
240	2075	2181	2308	3155	3325	3451	-27.4	-30.5	-29.4	-29.1	0.50	-135	-94	-123	-117	-108	-10
244	2122	2236	2371	3238	3416	3541	-27.4	-30.6	-32.0	-30.0	0.45	-143	-103	-122	-123	-107	-18
245	2134	2249	2387	3259	3439	3564	-26.0	-29.4	-30.6	-28.7	0.53	-155	-113	-134	-134	-109	-28
255	2257	2390	2558				-26.3	-29.7	-29.9	-28.6	0.54	-159	-118	-141	-139	-109	-34
260							-26.1	-29.8	-30.8	-28.9	0.52	-152	-113	-129	-131	-109	-26
265							-24.6	-28.4	-29.4	-27.5	0.61	-140	-90	-116	-115	-111	-5
270							-25.6	-29.1	-30.0	-28.3	0.56	-140	-100	-117	-119	-110	-10
275							-25.9	-29.5	-30.4	-28.6	0.54	-140	-90	-117	-116	-109	-7
280							-24.5	-28.4	-28.8	-27.2	0.62	-148	-84	-134	-122	-111	-12
285							-25.7	-29.2	-30.3	-28.4	0.55	-138	-92	-119	-116	-109	-8

CI, Confidence Interval

Table S2: Lake Salpeten Plant-wax Stable Isotope Data

Depth (cm)	TM Age 95% CI Lower	TM Age 'Best' (Yr BP)	TM Age 95% CI Upper	PW age 95% CI lower	PW Age 'Best' (Yr BP)	PW age 95% CI Upper	$\delta^{13}C$ C26 (‰)	$\delta^{13}C$ C28 (‰)	$\delta^{13}C$ C30 (‰)	$\delta^{13}C$ Mean (‰)	f_{c4}	δD C26 (‰)	δD C28 (‰)	δD C30 (‰)	δD Mean (‰)	ε_a (‰)	$\delta D_{wax\text{-}corr}$ (‰)
6.5	-50	-22	11	102	238	463	-30.6	-31.2	-30.9	-30.9	0.39	-137	-127	-139	-134	-105	-33
7.5	-46	-18	19	129	259	472	-29.6	-29.6	-29.7	-29.6	0.47	-138	-127	-154	-139	-107	-36
10.5	-34	-1	39	208	320	498	-29.6	-29.0	-28.3	-28.9	0.52	-130	-115	-124	-123	-108	-16
11.5	-29	5	48	234	341	506	-30.4	-29.3	-29.6	-29.8	0.47	-132	-118	-125	-125	-107	-20
12.5	-24	11	55	260	361	514	-29.4	-29.0	-29.8	-29.4	0.49	-136	-122	-130	-129	-108	-24
13.5	-19	18	64	284	381	523	-29.2	-29.5	-29.1	-29.3	0.49	-146	-125	-141	-137	-108	-33
16.5	-2	39	91	359	443	552	-30.2	-29.7	-28.6	-29.5	0.48	-148	-133	-141	-141	-107	-37
17.5	5	47	100	383	463	564	-29.6	-29.5	-29.7	-29.6	0.47	-153	-133	-154	-147	-107	-44
18.5	11	54	110	406	484	578	-30.9	-30.3	-29.5	-30.2	0.43	-137	-120	-129	-129	-106	-25
19.5	18	62	120	429	504	592	-29.8	-29.1	-28.7	-29.2	0.50	-141	-129	-130	-134	-108	-29
20.5	26	71	129	452	524	605	-29.1	-30.0	-29.8	-29.6	0.47	-147	-130	-143	-140	-107	-37
22.5	41	88	150	494	565	638	-30.0	-29.4	-28.8	-29.4	0.49	-136	-115	-124	-125	-108	-19
27.5	83	134	203	544	614	685	-29.3	-29.7	-28.7	-29.2	0.50	-154	-128	-150	-144	-108	-40
35.5	162	219	295	571	635	698	-29.5	-30.7	-30.2	-30.2	0.44	-151	-111	-151	-138	-106	-35
41.5	228	288	367	587	650	713	-28.1	-29.6	-28.2	-28.6	0.54	-152	-112	-152	-139	-109	-33
49.5	326	388	470	609	671	739	-28.7	-29.8	-29.1	-29.2	0.50	-141	-102	-135	-126	-108	-20
55.5	405	468	548	622	686	761	-28.0	-28.9	-28.8	-28.6	0.54	-125	-100	-115	-113	-109	-5
58.5	445	509	587	625	694	775	-28.9	-27.8	-27.7	-28.1	0.57	-127	-96	-109	-111	-110	-1
61.5	488	550	627	670	737	814	-29.4	-30.4	-31.1	-30.3	0.43	-146	-105	-126	-126	-106	-22
62.5	502	564	641	695	763	839	-28.3	-29.5	-30.4	-29.4	0.49	-140	-98	-110	-116	-108	-9
64.5	530	592	669	746	815	889	-30.4	-30.7	-31.7	-30.9	0.39	-133	-92	-92	-106	-105	-1
65.5	544	606	682	770	841	914	-29.5	-30.0	-31.0	-30.2	0.44	-151	-102	-123	-125	-106	-21
66.5	558	620	696	793	867	940	-30.5	-30.8	-31.4	-30.9	0.39	-133	-94	-96	-108	-105	-3
67.5	572	634	710	815	893	967	-29.9	-30.0	-30.0	-30.0	0.45	-128	-85	-82	-99	-107	9

Table S2 cont: Lake Salpeten Plant-wax Stable Isotope Data

Depth (cm)	TM Age 95% CI Lower	TM Age 'Best' (Yr BP)	TM Age 95% CI Upper	PW age 95% CI lower	PW Age 'Best' (Yr BP)	PW age 95% CI Upper	$\delta^{13}C$ C26 (‰)	$\delta^{13}C$ C28 (‰)	$\delta^{13}C$ C30 (‰)	$\delta^{13}C$ Mean (‰)	f_{c4}	δD C26 (‰)	δD C28 (‰)	δD C30 (‰)	δD Mean (‰)	ε_a (‰)	$\delta D_{wax\text{-}corr}$ (‰)
68.5	586	649	724	835	919	995	-29.2	-30.3	-29.0	-29.5	0.48	-138	-94	-101	-111	-107	-4
69.5	600	663	738	855	944	1024	-28.7	-30.2	-30.9	-29.9	0.45	-139	-94	-101	-111	-107	-5
70.5	614	677	752	875	970	1054	-29.4	-30.5	-30.4	-30.1	0.44	-143	-106	-121	-124	-106	-19
71.5	628	691	766	893	996	1085	-29.2	-30.7	-30.3	-30.1	0.45	-147	-107	-119	-124	-106	-20
72.5	642	706	779	912	1022	1116	-29.5	-29.8	-31.0	-30.1	0.44	-151	-111	-123	-128	-106	-25
73.5	656	720	793	931	1048	1148	-29.2	-30.4	-30.4	-30.0	0.45	-149	-111	-125	-128	-107	-24
74.5	670	734	807	949	1074	1180	-28.2	-29.7	-30.1	-29.3	0.49	-138	-94	-117	-116	-108	-10
77.5	712	778	849	1004	1152	1275	-30.0	-29.9	-31.4	-30.5	0.42	-110	-100	-108	-106	-106	0
82.5	784	850	916	1114	1267	1400	-29.0	-29.5	-31.3	-29.9	0.45	-174	-136	-144	-151	-107	-50
85.5	827	893	958	1178	1328	1458	-31.6	-30.0	-32.1	-31.2	0.37	-155	-113	-136	-135	-104	-34
86.5	841	907	973	1200	1348	1478	-29.4	-30.4	-30.9	-30.2	0.43	-154	-114	-126	-131	-106	-28
88.5	869	936	1001	1242	1389	1524	-29.8	-30.5	-31.1	-30.4	0.42	-134	-88	-106	-109	-106	-4
90.5	898	965	1030	1281	1429	1572	-30.3	-31.8	-32.6	-31.5	0.35	-141	-94	-111	-115	-104	-13
91.5	912	979	1043	1300	1449	1597	-28.5	-30.7	-31.0	-30.1	0.44	-147	-101	-116	-121	-106	-17
93.5	941	1008	1072	1334	1490	1652	-29.2	-30.0	-30.2	-29.8	0.46	-158	-114	-119	-130	-107	-26
95.5	970	1036	1102	1369	1530	1704	-31.3	-31.6	-31.2	-31.4	0.36	-152	-114	-130	-132	-104	-31
97.5	998	1064	1131	1396	1571	1758	-29.2	-29.5	-29.8	-29.5	0.48	-139	-108	-137	-128	-107	-23
99.5	1025	1092	1158	1424	1611	1818	-29.4	-30.1	-29.0	-29.5	0.48	-142	-100	-134	-125	-107	-20
100.5	1039	1106	1171	1437	1631	1847	-28.2	-30.7	-28.8	-29.2	0.50	-148	-112	-144	-134	-108	-30
101.5	1184	1124	1120	1452	1651	1876	-30.5	-31.2	-29.5	-30.4	0.43	-158	-118	-145	-140	-106	-38
102.5	1198	1138	1134	1463	1672	1905	-28.9	-30.3	-28.8	-29.3	0.49	-142	-111	-139	-131	-108	-26
104.5	1095	1162	1226	1489	1712	1964	-27.8	-30.0	-28.6	-28.8	0.52	-141	-115	-142	-133	-109	-27
105.5	1109	1176	1240	1502	1732	1995	-28.2	-29.5	-28.0	-28.6	0.54	-155	-126	-149	-143	-109	-38
111.5	1192	1257	1320	1643	1878	2146	-29.9	-31.1	-30.2	-30.4	0.42	-154	-116	-149	-140	-106	-38
112.5	1205	1270	1333	1678	1906	2167	-29.9	-32.0	-29.6	-30.5	0.42	-153	-121	-148	-141	-106	-39
114.5	1232	1297	1361	1747	1962	2208	-27.7	-29.9	-28.5	-28.7	0.53	-144	-110	-133	-129	-109	-23

Table S2 cont: Lake Salpeten Plant-wax Stable Isotope Data

Depth (cm)	TM Age 95% CI Lower	TM Age 'Best' (Yr BP)	TM Age 95% CI Upper	PW age 95% CI lower	PW Age 'Best' (Yr BP)	PW age 95% CI Upper	$\delta^{13}C$ C26 (‰)	$\delta^{13}C$ C28 (‰)	$\delta^{13}C$ C30 (‰)	$\delta^{13}C$ Mean (‰)	f_{c4}	δD C26 (‰)	δD C28 (‰)	δD C30 (‰)	δD Mean (‰)	ε_a (‰)	$\delta D_{wax-corr}$ (‰)
116.5	1257	1323	1387	1815	2019	2250	-27.7	-29.4	-28.6	-28.6	0.54	-164	-130	-153	-149	-109	-45
117.5	1270	1336	1400	1848	2047	2270	-29.7	-30.1	-29.5	-29.7	0.47	-162	-123	-149	-145	-107	-42
118.5	1283	1349	1412	1883	2076	2291	-29.0	-29.5	-29.7	-29.4	0.49	-155	-109	-137	-134	-108	-29
122.5	1332	1400	1462	2017	2189	2376	-29.5	-30.7	-30.0	-30.1	0.44	-163	-116	-140	-139	-106	-37
125.5	1368	1437	1499	2117	2273	2444	-28.1	-29.2	-28.7	-28.7	0.53	-161	-126	-146	-144	-109	-39
129.5	1417	1485	1556	2251	2387	2535	-28.5	-29.5	-28.9	-29.0	0.52	-155	-117	-135	-136	-108	-31
130.5	1426	1498	1561	2284	2415	2558	-31.4	-31.3	-31.5	-31.4	0.36	-155	-127	-141	-141	-104	-41
131.5	1437	1510	1573	2316	2443	2580	-29.4	-30.6	-29.1	-29.7	0.47	-147	-118	-141	-135	-107	-32
132.5	1448	1521	1586	2350	2471	2604	-30.3	-30.5	-29.8	-30.2	0.44	-138	-130	-150	-139	-106	-37
133.5	1460	1533	1598	2382	2500	2628	-27.3	-29.3	-28.8	-28.5	0.55	-150	-115	-136	-134	-109	-28
137.5	1499	1573	1639	2508	2613	2726	-29.2	-29.4	-28.6	-29.1	0.51	-155	-134	-151	-147	-108	-43
142.5	1558	1634	1702	2658	2754	2868	-27.6	-29.4	-28.3	-28.5	0.55	-150	-111	-131	-131	-109	-24
146.5	1601	1676	1745	2767	2867	2986	-29.8	-31.3	-29.8	-30.3	0.43	-154	-121	-136	-137	-106	-35
156.5	*1699*	*1776*	*1843*	*2794*	*2890*	*3009*	*-29.2*	*-31.0*	*-30.5*	*-30.2*	*0.43*	*-141*	*-110*	*-133*	*-128*	*-106*	*-24*
160.5	*1735*	*1812*	*1879*	*2798*	*2894*	*3012*	*-30.1*	*-31.8*	*-30.2*	*-30.7*	*0.40*	*-133*	*-106*	*-131*	*-124*	*-105*	*-20*
167.5	*1796*	*1873*	*1942*	*2805*	*2900*	*3019*	*-29.8*	*-31.5*	*-31.4*	*-30.9*	*0.39*	*-139*	*-108*	*-122*	*-123*	*-105*	*-20*
174.5	*1850*	*1929*	*2000*	*2810*	*2907*	*3027*	*-28.6*	*-30.6*	*-29.8*	*-29.6*	*0.47*	*-132*	*-102*	*-120*	*-118*	*-107*	*-12*
181.5	*1902*	*1980*	*2054*	*2814*	*2913*	*3032*	*-31.9*	*-30.9*	*-31.9*	*-31.6*	*0.35*	*-134*	*-113*	*-125*	*-124*	*-104*	*-23*
188.5	*1950*	*2027*	*2098*	*2819*	*2920*	*3038*	*-28.3*	*-30.7*	*-30.0*	*-29.7*	*0.47*	*-133*	*-110*	*-128*	*-124*	*-107*	*-19*
195.5	*1995*	*2070*	*2141*	*2823*	*2926*	*3046*	*-29.0*	*-31.3*	*-30.0*	*-30.1*	*0.44*	*-137*	*-107*	*-124*	*-122*	*-106*	*-18*
202.5	*2037*	*2109*	*2180*	*2827*	*2932*	*3056*	*-27.9*	*-30.3*	*-29.4*	*-29.2*	*0.50*	*-133*	*-107*	*-121*	*-120*	*-108*	*-14*
209.5	*2076*	*2146*	*2216*	*2831*	*2939*	*3066*	*-28.2*	*-30.5*	*-29.3*	*-29.3*	*0.49*	*-134*	*-113*	*-124*	*-123*	*-108*	*-17*
216.5	*2113*	*2179*	*2249*	*2834*	*2945*	*3076*	*-28.7*	*-31.0*	*-30.2*	*-30.0*	*0.45*	*-149*	*-122*	*-134*	*-135*	*-107*	*-32*
225.5	*2158*	*2220*	*2289*	*2838*	*2954*	*3091*	*-29.4*	*-31.7*	*-30.5*	*-30.5*	*0.42*	*-139*	*-114*	*-123*	*-125*	*-106*	*-22*
237.5	*2209*	*2272*	*2341*	*2844*	*2965*	*3112*	*-28.3*	*-31.0*	*-29.5*	*-29.6*	*0.48*	*-141*	*-100*	*-125*	*-122*	*-107*	*-17*
244.5	*2238*	*2302*	*2375*	*2846*	*2971*	*3125*	*-28.6*	*-30.3*	*-30.2*	*-29.7*	*0.47*	*-143*	*-94*	*-129*	*-122*	*-107*	*-17*

Table S2 cont: Lake Salpeten Plant-wax Stable Isotope Data

Depth (cm)	TM Age 95% CI Lower	TM Age 'Best' (Yr BP)	TM Age 95% CI Upper	PW age 95% CI lower	PW Age 'Best' (Yr BP)	PW age 95% CI Upper	$\delta^{13}C$ C26 (‰)	$\delta^{13}C$ C28 (‰)	$\delta^{13}C$ C30 (‰)	$\delta^{13}C$ Mean (‰)	f_{c4}	δD C26 (‰)	δD C28 (‰)	δD C30 (‰)	δD Mean (‰)	ε_a (‰)	$\delta D_{wax\text{-}corr}$ (‰)
251.5	*2268*	*2335*	*2408*	*2849*	*2978*	*3140*	*-30.5*	*-31.4*	*-32.4*	*-31.4*	*0.36*	*-128*	*-99*	*-111*	*-113*	*-104*	*-10*
259.5	*2305*	*2375*	*2451*	*2852*	*2985*	*3156*	*-28.4*	*-30.7*	*-29.4*	*-29.5*	*0.48*	*-145*	*-109*	*-131*	*-128*	*-107*	*-23*
265.5	2339	2409	2483	2948	3077	3245	-28.0	-29.9	-28.3	-28.7	0.53	-150	-121	-139	-137	-109	-31
269.5	2362	2434	2508	3056	3180	3340	-28.3	-29.5	-28.4	-28.8	0.53	-153	-120	-144	-139	-109	-34
272.5	2380	2453	2529	3137	3257	3412	-28.6	-31.0	-28.9	-29.5	0.48	-133	-92	-118	-114	-108	-8
276.5	2406	2481	2557	3245	3360	3507	-28.8	-30.0	-29.4	-29.4	0.49	-146	-106	-131	-128	-108	-22
279.5	2428	2504	2580	3325	3437	3579	-27.9	-29.9	-28.8	-28.9	0.52	-148	-106	-139	-131	-109	-25
283.5	2460	2536	2610	3432	3540	3675	-28.7	-29.9	-28.7	-29.1	0.51	-144	-100	-129	-124	-108	-18
286.5	2487	2562	2637	3513	3618	3750	-27.9	-30.3	-28.9	-29.0	0.51	-132	-91	-124	-116	-108	-8
288.5	2505	2580	2654	3567	3669	3800	-29.7	-31.3	-30.4	-30.5	0.42	-146	-111	-136	-131	-106	-28
290.5	2524	2599	2674	3621	3720	3852	-29.0	-29.4	-28.9	-29.1	0.51	-131	-113	-138	-127	-108	-21
293.5	2554	2630	2703	3700	3798	3929	-27.9	-29.1	-29.0	-28.7	0.53	-129	-87	-119	-112	-109	-3
297.5	2599	2673	2744	3805	3901	4037	-28.5	-30.1	-28.5	-29.1	0.51	-149	-120	-140	-136	-108	-31
301.5	2647	2720	2789	3911	4003	4148	-28.0	-30.4	-29.1	-29.2	0.50	-142	-103	-124	-123	-108	-17
304.5	2686	2759	2825	3989	4081	4232	-29.9	-30.2	-29.7	-29.9	0.46	-148	-122	-149	-140	-107	-37
307.5	2726	2799	2866	4067	4158	4318	-28.6	-31.0	-29.3	-29.6	0.47	-148	-118	-146	-137	-107	-34
311.5	2787	2858	2923	4170	4261	4432	-28.9	-29.9	-29.3	-29.4	0.49	-150	-111	-139	-133	-108	-29
314.5	2836	2905	2968	4248	4338	4517	-29.1	-31.0	-29.6	-29.9	0.45	-146	-105	-126	-125	-107	-21
323.5	3000	3064	3133	4480	4569	4775	-28.2	-30.3	-29.3	-29.2	0.50	-142	-101	-127	-123	-108	-17
328.5	3109	3169	3246	4606	4698	4919	-28.9	-30.1	-30.3	-29.8	0.46	-157	-112	-135	-135	-107	-31
335.5	3265	3325	3424	4781	4878	5115	-28.6	-29.6	-29.6	-29.3	0.49	-167	-102	-132	-134	-108	-29
340.5	3384	3453	3571				-28.1	-28.9	-28.4	-28.5	0.55	-163	-107	-136	-135	-109	-29
342.5	3433	3507	3629				-29.0	-29.3	-28.8	-29.0	0.51	-154	-109	-137	-134	-108	-28
348.5							-28.6	-29.4	-29.2	-29.1	0.51	-163	-101	-129	-131	-108	-26

Italics indicate core interval with minimal change in the PW age model. These data are not interpreted in terms of past environmental change.

CI, Confidence Interval

Table S3: Compound specific radiocarbon results from Lake Salpeten

NOSAMS sample number	Sediment Core Depth (cm)	$\Delta^{14}C_{wax}$ (‰)	error	2σ lower Cal age (Yr BP)	Median Cal age (Yr BP)	2σ upper Cal age (Yr BP)	$\delta^{13}C_{CO2}$ (‰)	$\delta^{13}C_{GC\text{-}IRMS}$ (‰)
88449	0.5-5.5	-8	18	-5	161	426	-32.9	
88551	23.5-25.5	-76	10	523	609	697	-32.8	
88453	59.5-60.5	-94	7	564	712	782	-29.5	
107434	75-85	-155	10	1058	1296	1362	-32.2	-31.9
88455	106.5-110.5	-212	14	1535	1866	2104	-28.4	
107435	143-150	-299	7	2780	2916	3057	-32.0	-31.7
107436	258-265	-300	9	2777	2990	3141	-31.9	-31.9
88463	338.5-339.5	-425	5	4853	4935	5256	-29.7	

Cal, calendar